Acta Geologica Polonica, Vol. 73 (2023), No. 2, pp. 201–222
DOI: 10.24425/agp.2022.143597

Interaction between tectonics, plutonism and mineralization of the Duna Pb-Ba ore deposit regarding fluid inclusion study (Central Alborz, Iran)

ALIREZA SADEGHI[1], SAEID HAKIMI ASIABAR[2]*, NIMA NEZAFATI[1,3], ALIREZA GANJI[2] and SOUMYAJIT MUKHERJEE[4]

[1] *Department of Earth sciences, Science and Research Branch, Islamic Azad University, Tehran, Iran; e-mails: asadeghi.1345@gmail.com; nima.nezafati@gmail.com*
[2] *Department of Geology, Lahijan branch, Islamic Azad University, Lahijan, Iran; e-mails: saeid.h.asiabar@gmail.com; ar_ganji2000@yahoo.com*
[3] *German Mining Museum, Department of Archaeometallurgy, Bochum, Germany; e-mail: nima.nezafati@bergbaumuseum.de*
[4] *Department of Earth Sciences, Indian Institute of Technology Bombay, Powai, Mumbai, Maharashtra, India; e-mails: soumyajitm@gmail.com, smukherjee@iitb.ac.in*
** Corresponding author*

ABSTRACT:

Sadeghi, A., Asiabar, S.H., Nezafati, N., Ganji, A. and Mukherjee, S. 2023. Interaction between tectonics, plutonism and mineralization of the Duna Pb-Ba ore deposit regarding fluid inclusion study (Central Alborz, Iran). *Acta Geologica Polonica*, **73** (2), 201–222. Warszawa.

This article discusses the impacts of overprinting of tectonic and plutonic events on the mineralization of the Duna Pb-Ba ore deposit, according to geologic settings and fluid inclusion studies. The Duna carbonate-hosted deposit contains a significant amount of Ag (18.9–264.3 ppm), Cu (77–41600 ppm), Sb (32.7–11000 ppm), Sr (63.5–15100 ppm), and Fluid inclusions with 7.34–23.65 wt.% NaCl equivalent. The homogenization temperature of about 110–285°C, as well as the paragenesis of the minerals shows a difference compared with other Pb-Zn deposits such as the Irish-type and MVT. The ore mineralization in the Duna mine occurred as stratabound, open space-filling, and along the brecciated fault zones. The concordant (stratabound) type of mineralization, with salinity and homogenization temperature of 18.54 to 23.65 wt.% NaCl equivalent, and 113°C to 165°C respectively, is usually typical of MVT-ore deposits, which in this area evolved during the Early Cimmerian orogeny and was later interrupted by mineralization along younger brecciated fault zones with salinity and homogenization temperature of 7.34 to 23.65 wt.% NaCl equivalent, and 113°C to 285°C respectively. This discordant mineralization, which occurred along the faults, formed by the end of the Late Cretaceous and during the Cenozoic as a result of the intrusion of a plutonic mass, and is comparable to the Irish-type ore deposits.

Key words: Alborz; Overprinting tectonics; Plutonism; Fluid inclusion; Structural control; Duna type ore deposit; Pb-Ba ore deposit; Carbonate-hosted.

INTRODUCTION

Because of the different opinions about the origin of Duna mine, such as a magmatic source for the mineralizing fluids (Samani-Rad 1999), a Mississippi Valley-type ore deposit (Yaghoob poor 2004), SEDEX (Bazargani-Guilani 1982), and a skarn type, or related to Tertiary magmatic activity (Hassanzadeh *et al.* 2002; Nekouvaght Tak *et al.* 2009), it was decided to conduct a more detailed investigation in Duna mine.

The Duna carbonate-hosted lead mine is located

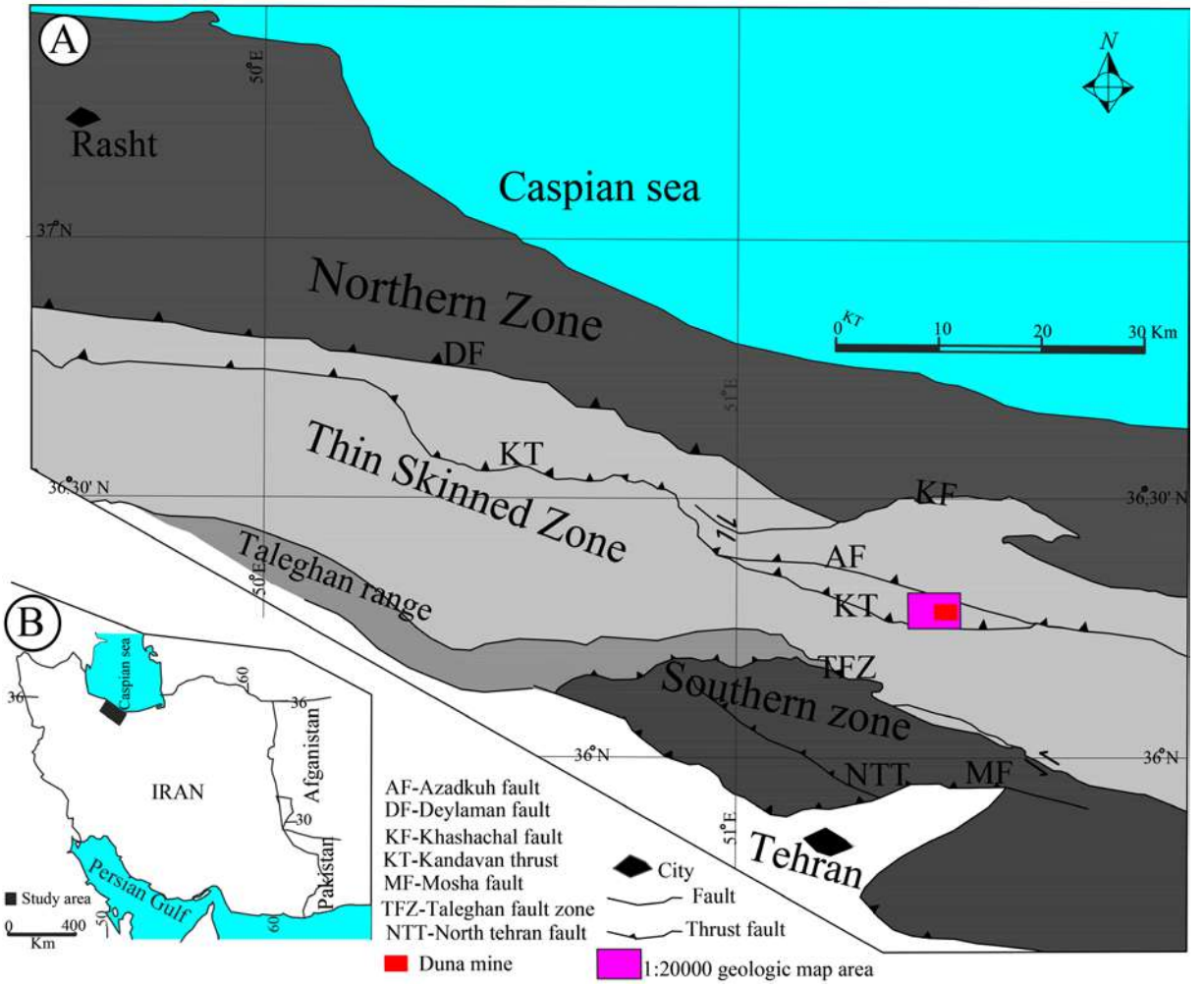

Text-fig. 1. A – Simplified tectonic zones of the Alborz structural zones of Iran, showing the location of the study area (modified after Guest et al. 2006). B – Location of the study area.

about 155 km north of Tehran, Iran (Text-fig. 1B) in the Central Alborz zone (Text-fig. 1A). The existence of different Pb, Zn, and Ba deposits such as Naserabad, Pachimiana, and Janatroodbar in the Central Alborz zone have made it one of the substantial disposed areas for exploring and mining activities, and Duna mine is one of the most complex deposits (Ghorbani 2013).

Several ore deposits in the Alborz range created by the end of the Cretaceous and during the Cenozoic (Mirnejad *et al*. 2015), are consistent with Laramide and Pyrenean Orogenic phases. However, in case of the Duna mine, Holzer and Momenzadeh (1969) consider this mineralization to be an example related to the Permian volcanogenics which originated in Central Alborz. Metals were thought to have been sourced from the Upper Paleozoic rock units of the Alborz range (Holzer and Momenzadeh, 1969; Samanirad 1999). In poly-orogenic systems, structural control of ore bodies often is not easy to understand, mostly because of multiple phases of mineralization, the relationship between structures, and ore bodies being indeterminate.

In this paper, we describe how new tectonic processes and intrusive masses affected the old mineralization such as MVT in the Duna mine. The fluid inclusion method was used in this investigation and these fluids helped to determine the type of mineralization in different mineralized faults.

MATERIALS AND METHODS

This study involves; (*i*) geometric modelling (system etc.) of deformation structures, *(ii)* study of min-

Sample	DSa1	DSa2b	DSa4	DSa7	DSa17	DSa8
Rock Type	Ore (dis)	Ore (con)	Ore (dis)	Ore (con)	Ore (con)	Brt (dis)
Ag	156.8	264.3	18.9	76	86.3	16.8
As	20.5	3328	49.7	12.9	39.3	34.9
Ba	9.545	24.50%	54.35	1232	1.20%	31.50%
Bi	0.6	0.8	0.2	0.3	0.7	0.25
Cd	12.6	57.4	13.7	<0.1	2.6	3.2
Cr	11	35	9	25	12	19
Cu	834	4.16%	497	77	203	244.5
Fe %	0.09	0.41	0.03	0.44	0.95	0.5
Mn	50	95	54	269	675	425
Ni	4	5	1	3	6	4.8
Pb	54.10%	347	3238	5731	38.50%	4660
S	10.80%	6.14%	13.10%	1121	5.71%	7.60%
Sb	566	1.10%	57.9	32.7	75	136.7
Se	2.81	5.53	1.01	0.68	0.59	0.4
Sn	0.6	0.7	0.5	0.8	0.5	0.55
Sr	501.3	1.20%	1.51%	65.3	400.6	1.30%
U	2.02	15.2	0.3	1	4.5	1.15
V	15	24	11	33	31	31
Zn	2188	1267	4170	10	94	581.5
Zn/(Zn+Pb)	0.01	0.79	0.57	0.01	0.0002	0.11

Table 1. The ICP-MS analysis results of the Duna mine samples in ppm; Brt – Barite; dis – discordant veins; con – concordant veins.

Sample code	N	Size (μm)	$T_{m\text{-}ice}$ (ºC)	$T_{m\text{-}HH}$ (ºC)	NaCl(wt. %)	NaCl+$CaCl_2$ (wt. %)	T_h (ºC)
DSa2a	2	–	-14.3	no	17.94	(<2)	132–134
DSa2b	17	5- 25	-11.5, -24	-25, -27	8.29, 22.2	18.54–28.78	106–197
DSa4	21	7- 25	-4.3, -23.5	-25, -34	3.96, 13.02	7.34–22.76	113–268
DSa8	24	10-80	-7.5, -20.5	-18,-23.5	9.05, 17.12	11.78–22.29	187–285

Table 2. Summary of the microthermometric data of the Duna mine. N – number of measurements; no – not observed; $T_{m\text{-}ice}$ – final ice melting temperature; $T_{m\text{-}HH}$ – final hydrohalite-melting temperature; T_h – homogenization temperature.

eralization forms in the field and in the laboratory, *(iii)* microthermometric investigations of fluid inclusions, and their geochemistry, and *(iv)* correlation of geologic events of the plutonic bodies based on the present field studies and the existing literature.

Field geology and sampling were conducted in three stages of summer and autumn 2017 as well as in summer 2018. Seven samples of concordant (Dsa2b, Dsa7, Dsa17) and discordant veins (Dsa1, Dsa4, Dsa8, Dsa14) of the Duna mine were selected for ICP-MS (Table 1) and microthermometric analyses (Table 2).

The samples were analyzed by the ICP-MS (Inductively Coupled Plasma-Mass Spectrometer) method using a PERKIN 9000 DRCE model in the Zarazma Mineral Studies Company, Iran following a near-total digestion applying four acid digestion including HF, HCl, $HClO_4$ and HNO_3. The steps of the sample preparation include drying at 120°C, crushing to less than 4 mm, pulverizing to 75 μm, analyzing under high temperature, and multi-acid digestion.

Microthermometric study of fluid inclusions in barite samples (DSa2a, DSa2b DSa4, and DSa8) was carried out using standard techniques (Steele *et al*. 2011), and a Linkam model THMS 600 heating-freezing stage mounted on a Zeiss, Axioplan 2, imaging microscope with a temperature range between -196ºC to +600°C, at the Mineral Processing Research Center (IMPRC) of Iran. This stage is equipped with two controllers, heating and cooling. The accuracy is estimated to be ±0.2ºC on freezing (-94.3ºC) and ±0.6ºC on heating (melting point: +414ºC). The correlation of the tectonostratigraphic chart, and the crosscutting relationships between faults and veins helped us to understand the relative age data of geologic events. Four phase-change points of the fluid inclusions were measured: freezing (Tfz), first melting temperature (Tfm), melting point of hydrohalite (Tm-HH), and last ice-melting temperature (Tm_{ice}). Most samples contain numerous liquid-vapor types of fluid inclusion that homoge-

nized in the liquid phase. The freezing temperature deals with the temperature at which the solution suddenly darkens or the vapor bubble instantly deforms at the time of the cooling process. The first melting point displays the temperature of the frozen solution (generally dark) on which the fluid abruptly brightens during heating. This is the start melting point of the solid assemblage.

GEOLOGICAL SETTING

The Central Alborz zone (Text-fig. 1A) is divided into the Northern Alborz zone, the Thin-skinned zone, Taleqan range, and the Southern Alborz zone (Guest *et al*. 2006). The Duna Pb-Ba ore deposit is located around the northern border of the Thin-skinned zone. In the northern zone, deformation appears to intensify southward-from the northern foothills to the range crest. This zone is composed of W-E striking faults and folds. The Northern zone deformed during the Laramide orogeny (Hakimi Asiabar and Bagheriyan 2018). The Thin-skinned zone is bounded by the Northern Alborz zone to the north and the Taleghan fault zone (TFZ) to the south. Most of the Taleghan range is comprised of a large, open, upright, gently west-plunging anticline with its limbs truncated by the high-angle Taleghan fault zone along its northern flank, and by the Mosha thrust, along its southern flank (Guest *et al*. 2006). The Southern zone comprises NW-SE trending thrusts, synclines, and anticlines, which were refolded, and formed an older set of folds that trend roughly northeast-southwest (Guest *et al*. 2006). Some observations imply that the entire Southern folded zone is a large transpressional duplex system (Guest *et al*. 2006).

In the central Alborz zone, the Paleozoic and Mesozoic rocks are covered by volcanic and pyroclastic Cenozoic rocks. The area of Duna Pb-Ba mine consists of Paleozoic rocks overlain by Quaternary deposits (Text-figs 2–4). The Paleozoic units are composed of black dolostones (Durod Formation), light grey limestones (Ruteh Formation), and andesitic basalts and shales of the Nessen Formation. Near to the mining area, the Mesozoic rock units of the study area are present (Text-fig. 3). These commence with the grey dolomitic limestone and creamy dolostone of the Triassic Elika Formation (Aghanabati 2005). The Shemshak Formation, which is the main coal-bearing sequence of the Alborz range, was deposited unconformably over the Triassic Elika Formation during the Upper Triassic–Lower Jurassic (Aghanabati 2004). In the uppermost part of the Shemshak Formation, just 3 km west of the mining area, limestone beds of the Delichai and Lar formations crop out with the presence of marine fauna.

Numerous normal faults in the Jurassic rock units in the Northern Alborz zone indicate that these rock units have formed in a subsidence area such as a rift valley basin (e.g. Allen *et al*. 2003; Hakimi Asiabar and Bagheriyan 2018). The southern side of the Kandavan fault, with its relatively thinner sequence,

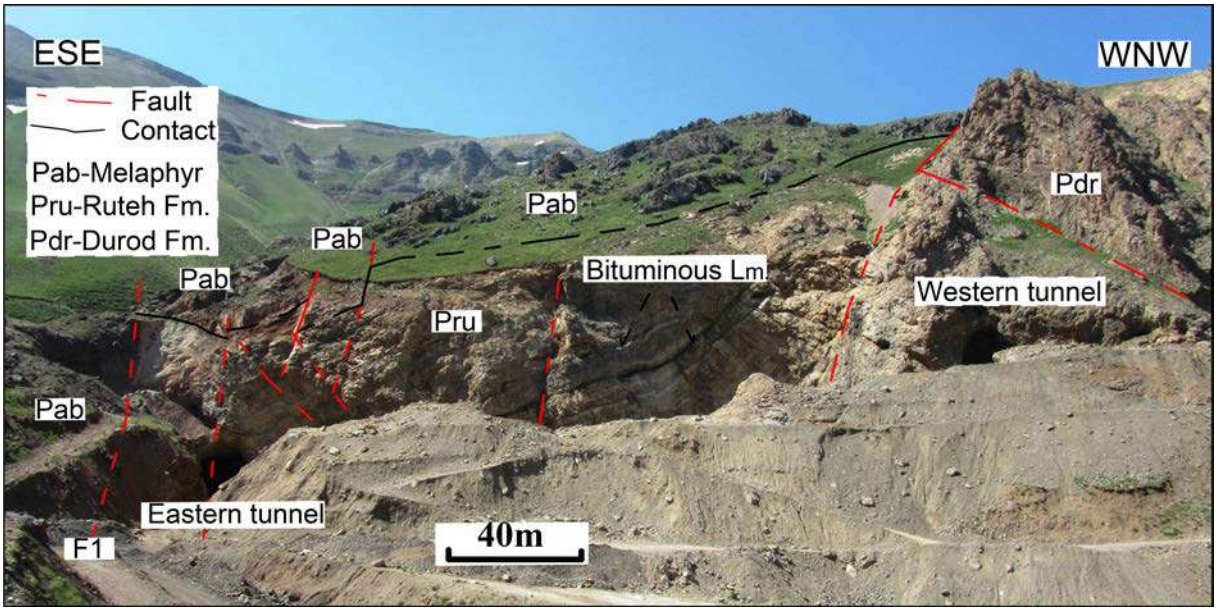

Text-fig. 2. View of the tunnels in the eastern part of Duna mine with bituminous limestone (Lm.) layers and reverse fault F1 shown in Text-figs 3 and 4.

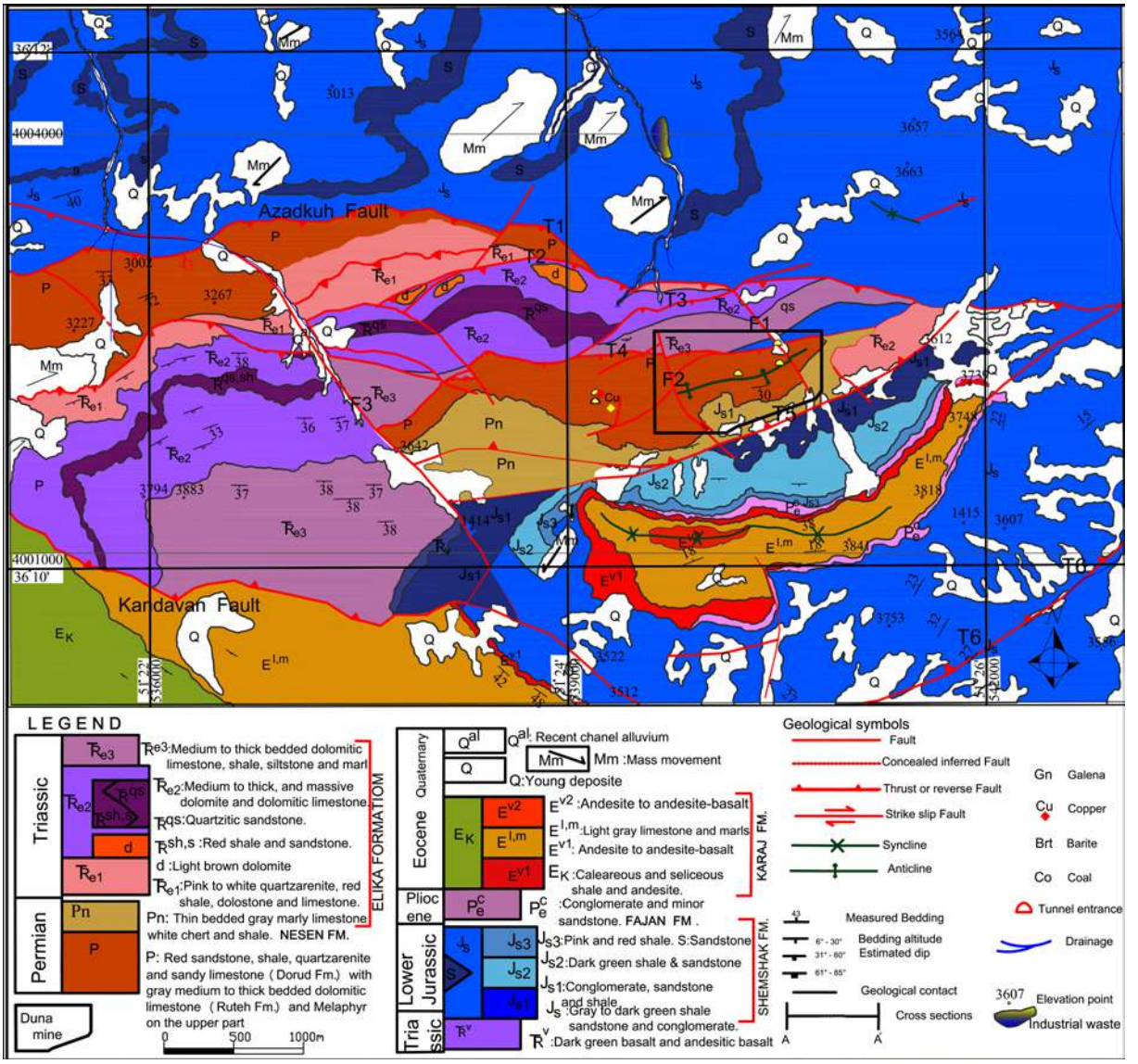

Text-fig. 3. Geological and structural map of the Duna area (modified after Hakimi Asiabar 2019), showing the location of the study area.

probably was one of the margins of a rift valley system. The Late Cimmeride event created the angular unconformity between Jurassic and Cretaceous sediments seen in the Thin-skinned and the **S**outhern folded zones of the Alborz range (Baharfiruzi and Shafeii 2005). Lower Cretaceous sedimentation commenced with the deposition of Orbitolina-bearing limestones (Tizkuh Formation) with a coarse-grained conglomerate at the base in some areas and continued with the volcanic eruptions and pelagic limestones of the Upper Cretaceous with more subsidence in the Northern Alborz zone (Annells 1975; Baharfiruzi and Shafeii 2005). The sedimentary rock units of the northern side of the study area, during the Upper Cretaceous, began with benthic limestones and gradually changed into hemipelagic to pelagic sediments (Modaresnia *et al*. 2012), which were accompanied by eruptions of more than 2000 m thick dark-grey to black, basic to intermediate volcanic and pyroclastic rocks (Baharfiruzi and Shafeii 2005). Overall, the volcanic rocks in the Upper Cretaceous show epicontinental to continental and oceanic successions respectively from the south to the north (Hakimi Asiabar and Bagheriyan 2018).

The Paleogene rock units are composed of several consecutive volcanic phases that overlapped onto older formations with a remarkable unconformity (Aghanabati 2005**)**. Neogene sediments crop

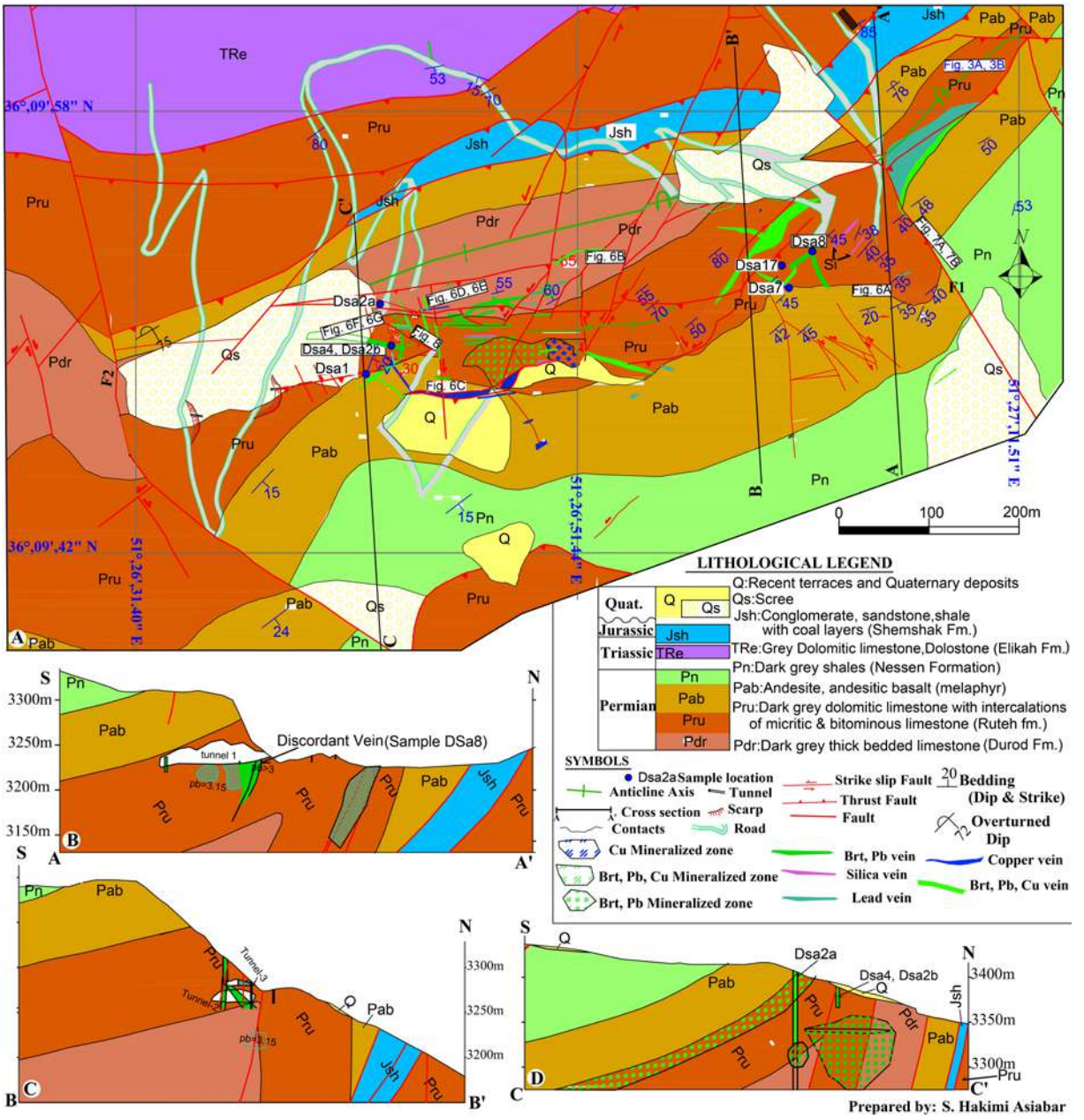

Text-fig. 4. A – Geological map of the Duna mine showing the small-scale faults and sampling locations. B, C, D – structural cross-sections of the Duna mine (Hakimi Asiabar 2019).

out in the intermontane basins and in the southern vicinity of the Duna anticline (Hakimi Asiabar and Bagheriyan 2018), including red-conglomerates and fine clastic deposits. This sequence lies unconformably on the Paleogene volcanic and sedimentary rock sequences. Quaternary deposits are widespread on the Caspian plain, and are preserved as patches in many places, and intermountain basins. Eocene plutonic rock units are intruded into the Mesozoic rock units of the study area. The few normal faults of the Alborz range trend east-west (Axen *et al*. 2001). The Alborz compression range underwent an inversion tectonics style of deformation (Zanchi *et al*. 2006; Ehteshami-Moinabadi 2016) during the Mesozoic and Cenozoic, and parts of its displacement occurred along strike-slip faults (Jackson *et al*. 2002; Allen *et al*. 2003). Researchers (e.g., Guest 2004; Guest *et al*. 2006) have confirmed that the reactivation of the

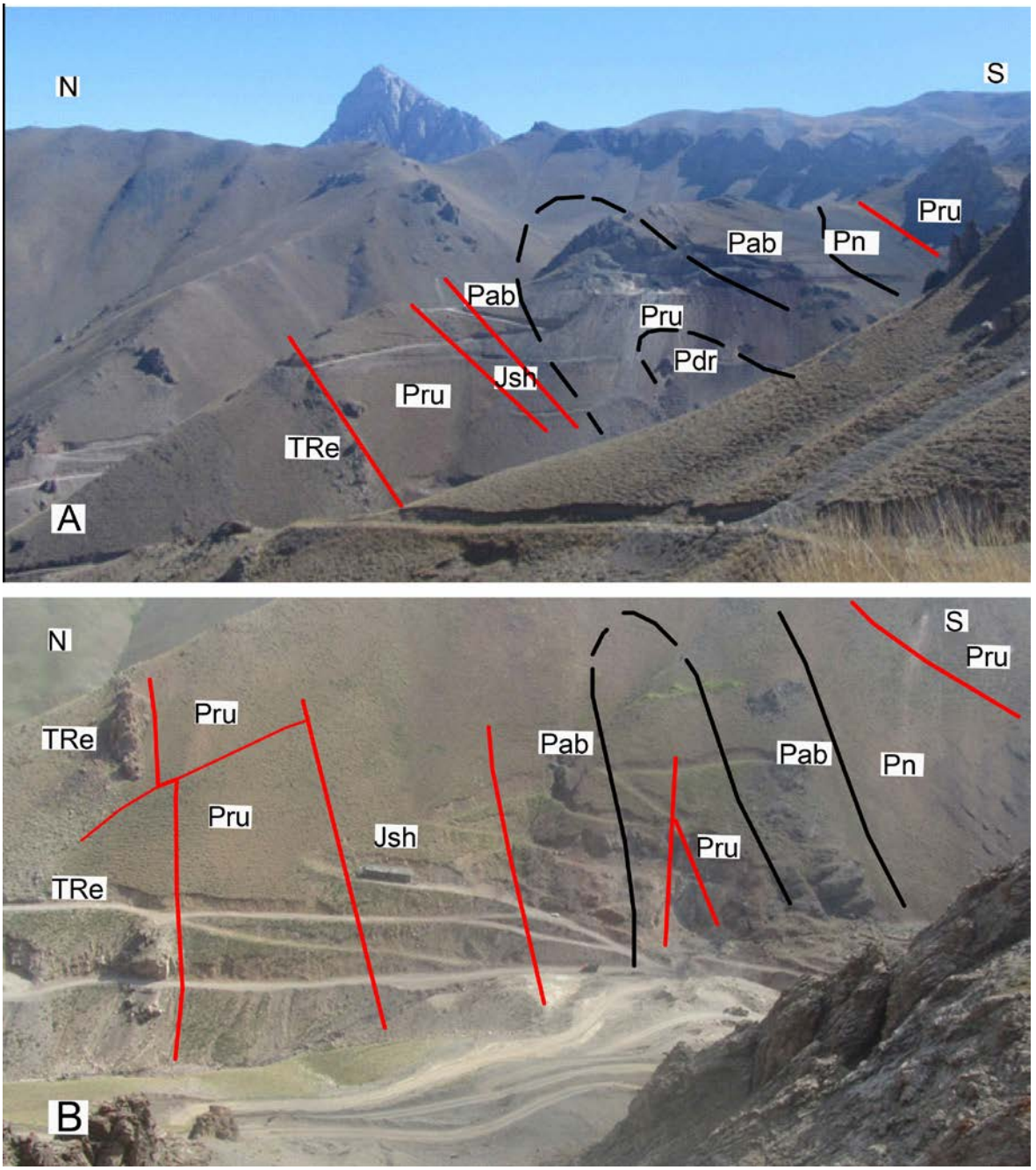

Text-fig. 5. A – Overturned folding in the Duna anticline (view to the east). B – Isoclinal fold in the eastern side of the Duna mine (view to the east). Abbreviations: Jsh – Jurassic Shemshak Formation; Pab – Permian Melaphyr; Pdr – Permian Durod Formation; Pn – Permian Nessen Formation; Pru – Permian Ruteh Formation; Tre – Triassic Elika Formation.

Late Cretaceous oblique-slip thrust faulting occurred possibly as late as 7 Ma, possibly due to the Late Neogene onset of continental collision.

About 56 ± 2 Ma, the Akapol granitic body of Central Alborz was intruded in the Middle Paleocene (Allen *et al.* 2003) in the western part of the study area. The crystallization and thermal histories of the Akapol and Alamkuh plutons obtained by U/Pb, $^{40}Ar/^{39}Ar$ (Axen *et al*, 2001b), and (U-Th)/He analyses of zircon, biotite, k-feldspar, and apatite, prove that the Akapol granitoid was intruded at 56 ± 2 Ma. Petrologically, the Akapol granitoid intrusion with

~50 km^2 area contains two categories of felsic (granite, quartz monzonite and quartz syenite) and intermediate to mafic rocks (monzonite-monzodiorite, diorite and gabbro). The monzonite and monzodiorite rocks of this granitoid show the properties of high-temperature, I-type granites, which can be categorized as post-orogenic granites. The felsic rocks of the Akapol granitoid intrusion show the properties of low-temperature, I-type granites (Sajadi Nasab *et al*. 2014).

The main geological structures and faults

Geological maps with a scale of 1:20000 (Text-fig. 3) and 1:1000 (Text-fig. 4), and structural cross-sections (Text-fig. 4B–D), illustrate an overturned anticline in Duna mine (Hakimi Asiabar 2019). The Azadkuh fault is located ~ 300 m north of the Duna Pb-Ba ore deposit (Text-fig. 3) with a length of ~30 km and a dip of 20–25° to the south (Hakimi Asiabar and Bagheriyan 2018). The Permian and Triassic rock units are thrusted over the Jurassic rock units by the Azadkuh fault. The E-W striking ~300 km long Kandavan fault is located ~2.5 km south of the Duna mine. The dip of the Kandavan fault is ~45° to the north and it thrusts the Paleozoic rock units over the Neogene rocks (Hakimi Asiabar and Bagheriyan 2018).

The tectonic style of the Alborz range is dominated by thrust faults with a nearly W-E trend. The Duna mine situated in the core of an overturned anticline with WSW-ENE trend (Text-fig. 4), which is inclined towards the north (Cross-section AA', BB' in Text-figs 4, 5A). As a part of a pop-up structure, this gently (~15°) east-plunging, tight anticline is located between the Kandavan and the Azadkuh thrust faults. The axis of the Duna anticline is ~6 km long, and the Durod and Ruteh Formations (cross-sections in Text-fig. 4) are the oldest units of this anticline (Hakimi Asiabar and Bagheriyan 2018).

The Duna mining site is divided into the eastern, middle, and western blocks by F1 and F2 faults (Text-figs 4 and 5). Faults F1 and F2 are important faults with ~N30W to N40W strike and >75° dip to the west, and the anticline has become isoclinal due to compression (Text-fig. 5B). As a result of this compression, numerous faults have been created in the core and flanks of the anticline.

There is a network of brittle shear zones comprised of breccia, cataclastic rocks, and gouge with meso-scopic indicators, e.g., slickensides, slickenfibers, and mineral lineations (Mukherjee 2013, 2014, 2015) in the Duna ore deposit. According to the cross-cut relationships (T1, T2, T3, T4, and T5; and F1, F2, and F3 in Text-fig. 3, the thrust faults of the study area can be divided into the three following generations from the oldest to youngest. The first generation of thrust faults with WSW-ENE trend, strike dip 40–50° (slip rake angle more than 60° to SE), which were formed during folding (Lisle 1986; Mitra 2003; Aerden *et al*. 2010), and progressive deformation. Around 65% of these faults hold mineralization in their brecciated zones (Text-fig. 6B, D). Most of the first-generation thrust faults crop out on the overturned layers of the Duna anticline (Text-figs 2, 4), and some of these faults have a flexural shape or curvatures in plain view (Text-figs 4, 5), but in general they are parallel the bedding trace (Text-fig. 7A) and trend of the fold axis (Text-fig. 4). The second group is a fault set with a nearly E-W trend and reverse slip sense (rake of slip vector <50° to SE), and is diagonal to the fold axis of the Duna anticline and the bedding (Text-fig. 7B). This fault set intersects the first generation of fault arrays at ~10–15°, and is of secondary importance for mineralization. Around 45–55% of this fault array has mineralized zones (Text-fig. 6E, F). The third category of faults with a nearly N30W to N40W trend, dip more than 75° to the southwest, intersecting the first and second fault sets (see F1, F2, and F3 in Text-figs 3, 4, and 7C, D). The altitudes of F1 (Text-figs 2, 3), and F2 are N35W/79SW and N39W/60SW, with a measured net-slip of ~41 and 39 m, respectively. Most of this category of faults don't have mineralization (Hakimi Asiabar 2019).

RESULTS

Fluid inclusions

Petrographic and Microthermometric studies of fluid inclusions were carried out on barite from concordant (DSa2a and DSa2b), and discordant veins (DSa4 and DSa8). Table 2 presents the microthermometric outcomes.

The first melting temperature (Tfm) for all fluid inclusions is -55ºC to -45ºC, and corresponds to the eutectic temperature for all fluid inclusions, which is related to the salt system NaCl+$CaCl_2$ and KCl (Shepherd *et al*. 1985). The melting point of hydrohalite (Tm-HH) has a range of -27°C to -25°C, which is the result of NaCl concentration into soluble salts of different ratios of NaCl/NaCl+$CaCl_2$, and up to -34°C, which in turn indicates the presence of Ca^{+2} cations in the fluids (Goldstein and Reynolds 1994). The temperature of final ice melting (Tm-ice) ranges from -24ºC to -4.3ºC. The relationship between last ice melting and salinity

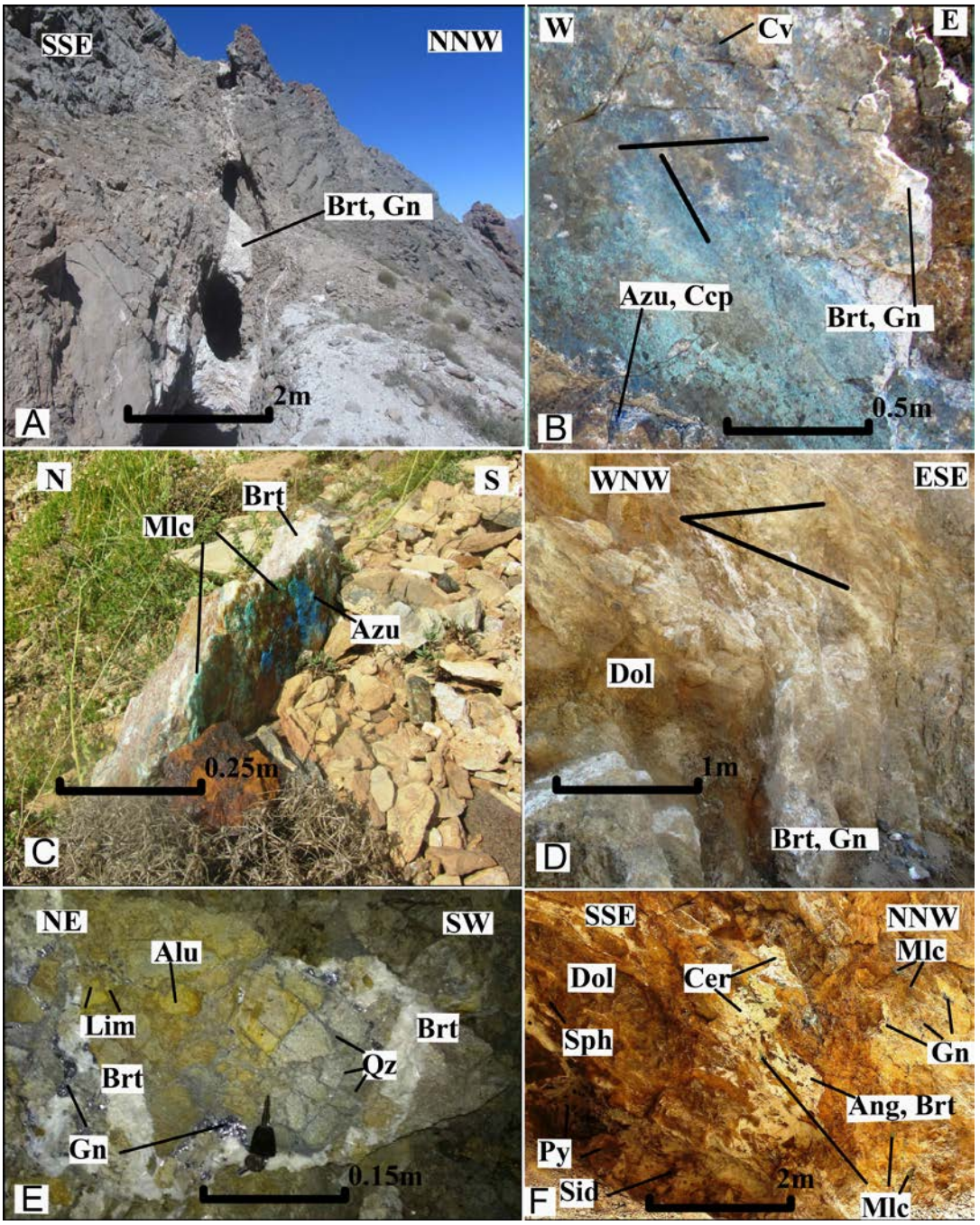

Text-fig. 6. A – Galena and barite deposited along a fault zone. B – Breccia zone include; malachite, chalcopyrite, covellite, and main mineralized barite and galena. C – Malachite and azurite and barite in the dolomite host rock. D – Barite and galena intergrowth in dolomite. E – Galena and barite deposited as open space filled with alunite, limonite and quartz of the breccia zone. F – Mineralized brecciated limestone. Abbreviations: Alu – Alunite; Ang – Anglesite; Azu – Azurite; Ba – Barite; Ce – Cerrucite; Co – Covellite; Ccp – Chalcopyrite; Dol – Dolomite; Gn – galena; Lim – Limonite; Mlc – Malachite; Py – Pyrite; Sid – Siderite; Sph – Sphalerite; Qz – Quartz. Symbols from Laurence (2021).

(wt.% NaCl eq.) shows the salinity of the ore-forming fluids (Sephered *et al*. 1985; Sadeghi *et al*. 2022).

Some of the fluid inclusions are in elongate and regular polyhedral shapes, which probably indicates the tectonic stresses in the area (Hashemian *et al*. 2018; Sadeghi *et al*. 2022). The fluid inclusions of the discordant veins are larger (7–80 μm) than those of the concordant veins (5–25 μm). Liquid-vapor (L-V),

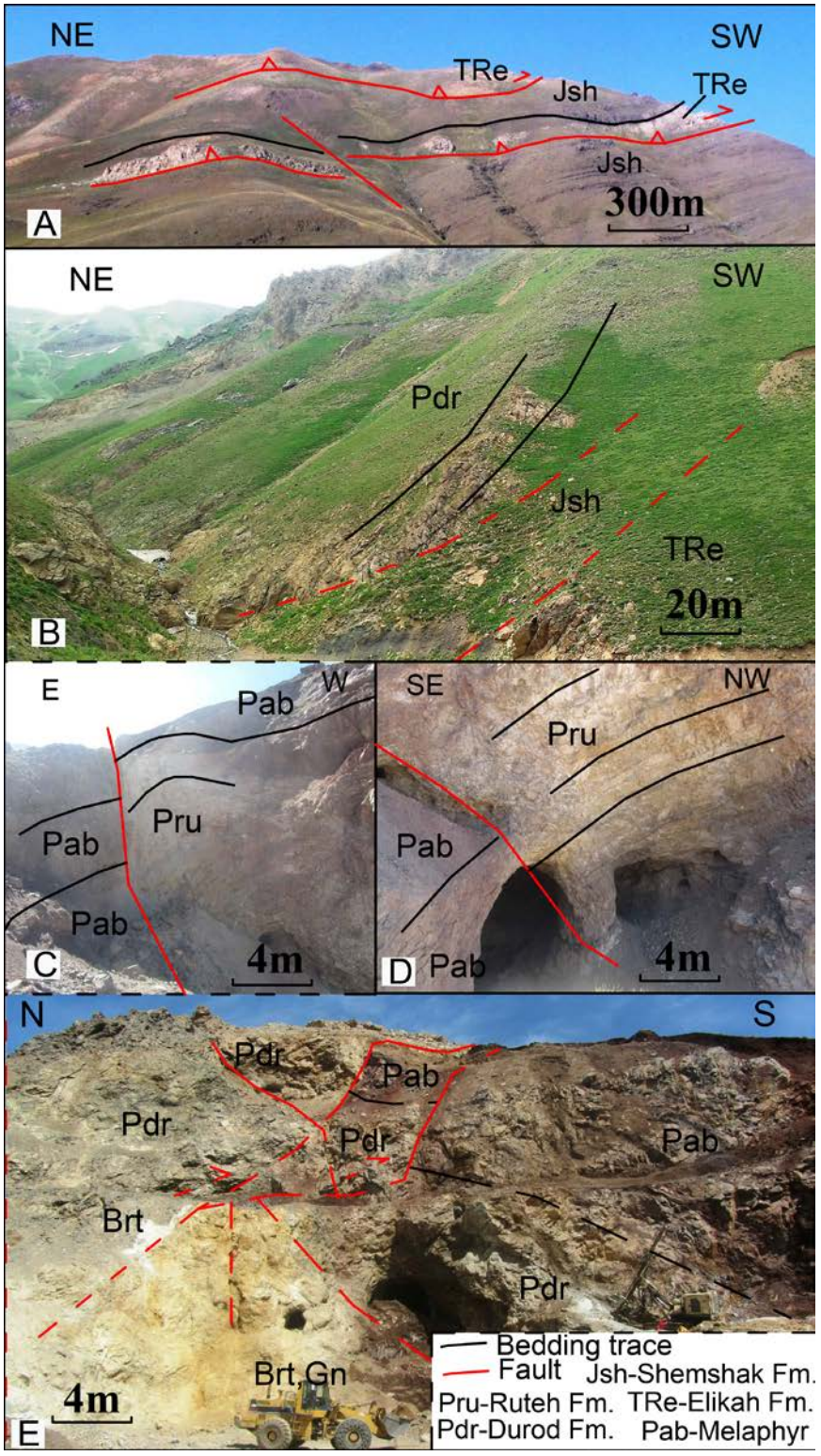

Text-fig. 7. A – Outcrop of Azadkuh fault (View to the southeast), which shows overriding Ruteh Formation (Pru) on Shemshak (Jsh) and Elika (Tre) Formations. B – Outcrop of the thrust fault, which is diagonal to the bedding surface. C – The outcrop of fault F1 (view to the south). D – Strike-slip fault with mineralization on the top levels of Ruteh Formation (view to the east). E – Strike-slip fault with mineralization of barite and galena in Durod and Ruteh formations on the border of Melaphyr unit (Pab). Abbreviations: Ba – Barite; Gn – galena (symbols from Laurence 2021).

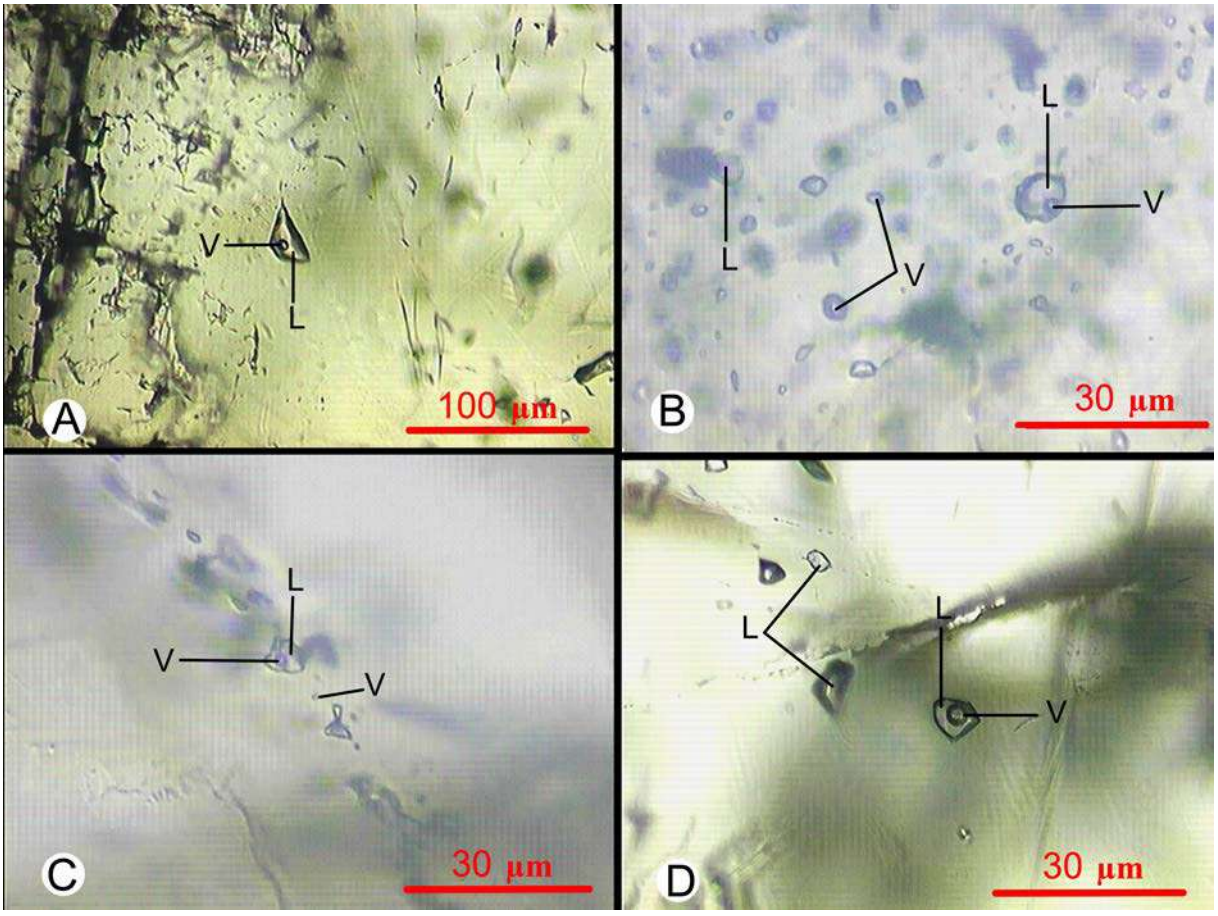

Text-fig 8. A – Necking down in fluid inclusion hosted in barite of DSa2a; B – Fluid inclusions of two-phase liquid and vapor (L+V), mono-phase liquid (L), vapor (V) in DSa8; C – Linear arrangement of Fluid inclusion hosted in barite of DSa4; D – Linear arrangements of Fluid inclusion in barite of DSa8.

and less common mono-phase liquid (Text-fig. 8A) types of inclusions are distinguished in concordant veins, while discordant veins (Text-fig. 8B, C) are comprised of three types of inclusion: mono-phase liquid (L), vapor (V), and liquid-vapor (L-V). The presence of mono-phase gas can indicate inclusion opening by a fracture due to the perfect cleavage of barite as a result of pressure reduction at the fractures and faults during discordant-veins mineralization in the Duna mine (Sadeghi *et al*. 2022). The fluid inclusions are of primary origin but many fluid inclusions in micro-cracks cutting with linear arrangement in different directions (Text-fig. 8C) can indicate the secondary origin or the next generation of the inclusions as a result of stress and various tectonic activities (Sadeghi *et al*. 2022) and indicates two stages of mineralization in the Duna mine.

A total of 64 fluid inclusions ranged from 7.34 to 23.65 wt.% NaCl equivalent, and they homogenized between 113 and 285ºC, and the liquid/vapor ratio is 70 to 80.

The salinity and homogenization temperature of fluid inclusions in concordant veins changes between 18.54 and 23.65 wt.% NaCl equivalent, and in the ranges 135–165ºC, and in discordant layers, between 7.34 and 22.76 wt.% NaCl equivalent, and in the ranges 113–285ºC respectively (Text-fig. 9B). This variety of salinity is due to the different origins of fluids or combination of several fluids types (Wilkinson 2001), and the high homogenization temperature in barite seems to be acceptable due to the lack of leakage and bursting of the inclusions. To ensure the absence of leakage in fluid inclusions, a thermometer test was performed with great long time and repetition (Sadeghi *et al*. 2022).

The plot of Duna Pb-Ba ore deposit fluids falls within the Irish type mineralization (Text-fig. 9A), which in turn is a kind of Mississippi Valley Type

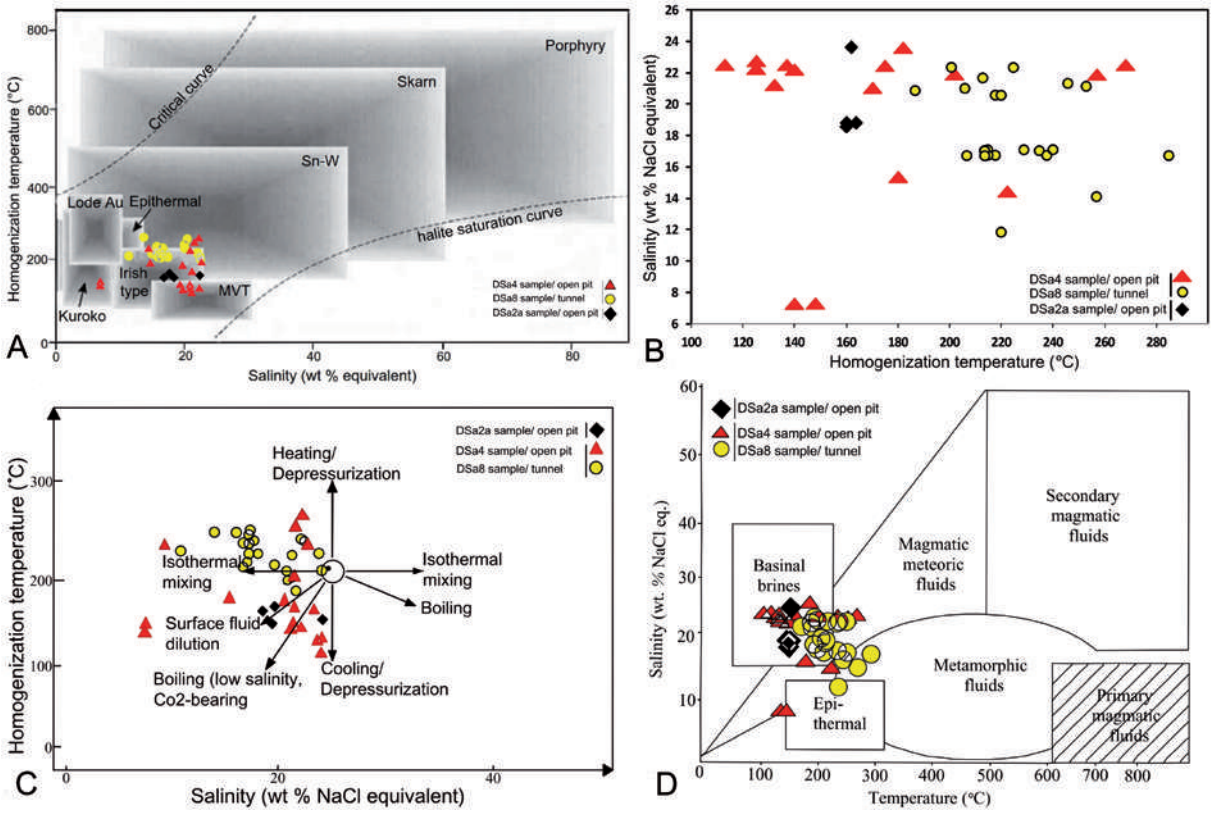

Text-fig. 9. A – Homogenization temperature-salinity plot for fluid inclusions (Roedder 1984) from ore sample of open pit and massive barite of tunnel for MVT (DSa2a), and Irish-type (DSa4 and DSa8) of mineralization in the Duna mine. B – Homogenization temperature-salinity plot for fluid inclusions from ore samples of concordant vein (DSa2a), and discordant veins (DSa4 and DSa8) in the Duna mine. C – A schematic diagram showing typical trends in homogenization temperature-salinity space due to various fluid evolution processes (Wilkinson 2001), and position of ore-bearing fluids for MVT (DSa2a/open pit), and Irish-type (DSa4/open pit and DSa8/tunnel) of mineralization in the Duna mine. D – A homogenization temperature-salinity diagram (Bean 1983) for ore-bearing fluids from open pit/1st stage/older/MVT (DSa2a), and discordant veins/second stage/younger/Irish-type (DSa4 and DSa8) in the Duna mine.

(MVT). As per Text-fig. 9C (Wilkinson 2001), cooling pressurization and surface fluid dilution are evident in the veins of the Duna Pb-Ba ore deposit. The homogenization temperature-salinity diagram for ore-bearing fluids (Beane 1983), indicates the involvement of basin brine fluids in concordant veins (DSa2a), and magmatic-meteoric fluids in discordant veins (DSa4 and DSa8) in the Duna mine (Text-fig. 9D).

Mineralogical characteristic

The ore mineralization in the Duna mine occurs as stratabound, open space-filling in the form of dolomitic alteration zones (Samanirad 1999; Rajabi *et al*. 2013), and along brecciated fault zones. According to the microscopic and macroscopic studies, galena is the main ore mineral while sphalerite, pyrite, and chalcopyrite comprise the accessory ore minerals. Galena occurs paragenetically with tetrahedrite. Barite, dolomite, calcite, and quartz are gangue minerals. Supergene minerals include covellite, cerussite, anglesite, malachite, and azurite, which are accompanied by Fe-Oxy-hydroxides, alunite, and clay minerals. The paragenetic sequence of the Dune Pb-Ba mine is shown in Text-fig. 10.

Microscopic study of the samples collected from both concordant and discordant veins mineralization (Text-figs 11, 12), demonstrates two stages; mineralization in the first (older) stage of the Mississippi Valley-type (low temperature), and no magmatic activity, and mineralization in the second (younger) stage of Irish-type (high temperature), and probably with magmatic activity (Sadeghi *et al*. 2022). Galena is seen both undisturbed and altered from the margins into covellite and cerussite (Text-fig. 11A, E). Coarse crystalline euhedral galena and barite crystals are generally restricted to fracture-fill mineralization or vugs within the main ore-stage assemblages, where

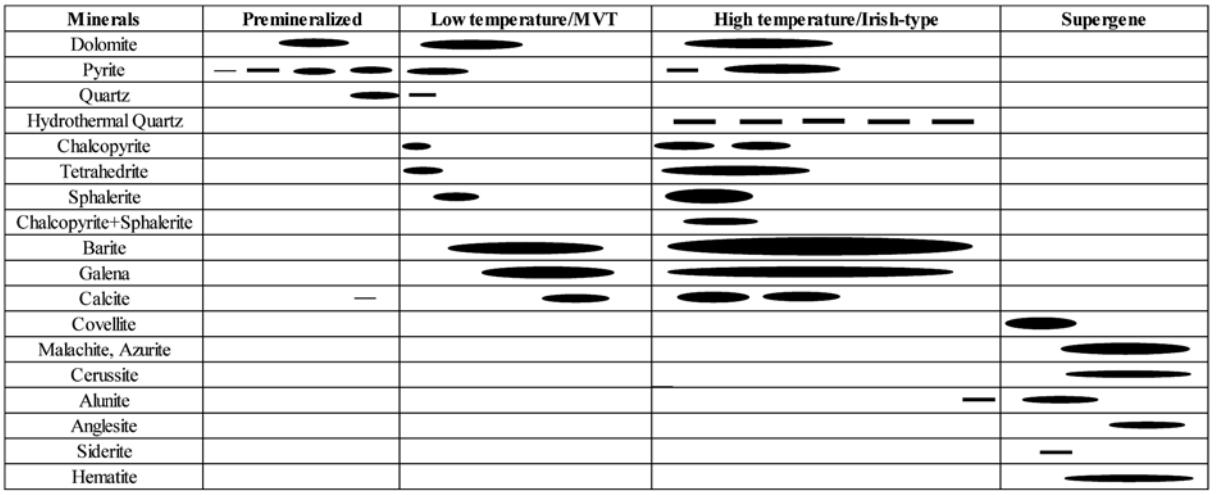

Text-fig. 10. Summary of paragenetic sequences of mineralization in the Duna mine.

they occur along with euhedral dolomite and calcite (Text-fig. 11A, B, E). Galena's curved shape in some microscopic sections (Text-fig. 11C) is a sign of mechanical (tectonic) pressures on the rock after the formation of the ore mineral. Galena at the main stage is accompanied by inclusions of sphalerite, tetrahedrite, chalcopyrite and pyrite, which shows open space filling texture (Text-fig. 12). Co-precipitation of sphalerite and chalcopyrite (Text-fig. 12B) is formed in the second stage (e. g. sample DSa4) of mineralization. Quartz is usually found in the hydrothermal breccia and brittle shear zones of discordant veins and probably confirms the hydrothermal origin of some fluids (Text-figs 6E, 11B).

Copper minerals are minor constituents of mineralization and are absent in some of the principal lodes.

Mineral composition of Ore deposit (vol %)		
Pb minerals	galena	3–6
	anglesite	<0.2
	cerrucite	<0.3
Zn minerals	sphalerite	1
Cu minerals	chalcopyrite	0.7–0.9
	malachite, azurite	<0.3
	covellite	<0.1
	tetrahedrite	<0.1
Main Gangue	barite	55–60
	quartz	8–10,
	calcite and dolomite	15–20
	pyrite	0.50
	siderite	<0.5
	FeOx	<2

Table 3. The main mineral content of Duna mine according to field observations.

Increasing hydraulic pressure caused hydrothermal fracturing and the origin of breccia (Text-fig. 6E), and three kinds of mineral alterations in the brecciated zones. Field observations as well as mineralogical and petrographic studies show dolomitization, silicification and haematitisation of the host rock. Dolomite as a gangue mineral emerged during dolomitization before the main mineralization stage. Silicification and haematitization are usually accompanied by hydrothermal fluids in the main mineralization and supergene stage respectively (see Text-fig. 13) . The galena evolved during the low and high temperature stages of mineralization (see Text-fig. 10).

The distribution of minerals and the grade of Pb, Zn, Cu, and Ag in the deposit are non-uniform. Veins are composed of several minerals (Text-figs 6A–F, 13). Table 3 presents the mineral frequency in veins and mineralized zones from outcrops in several excavated tunnels, and open-pit areas. In many discordant veins that developed along the strike-slip and thrust faults, barite is the most common mineral, occurring as large euhedral crystals with ~55–60% mineralization formed within open cavities (Hakimi Asiabar 2019).

Faults and mineralization

The distribution of mineralized zones in Duna anticline with ~WSW-ENE trend coincides with the main axis of the proposed basin (Guest 2004), and can be assumed regionally. Some of the mineralized zones evolved discordantly in the core of the Duna anticline and in the brecciated zones of strike-slip and thrust faults (Text-figs 3, 4, 6). According to the tectonostratigraphic sequence (Axen *et al*. 2001b; Allen

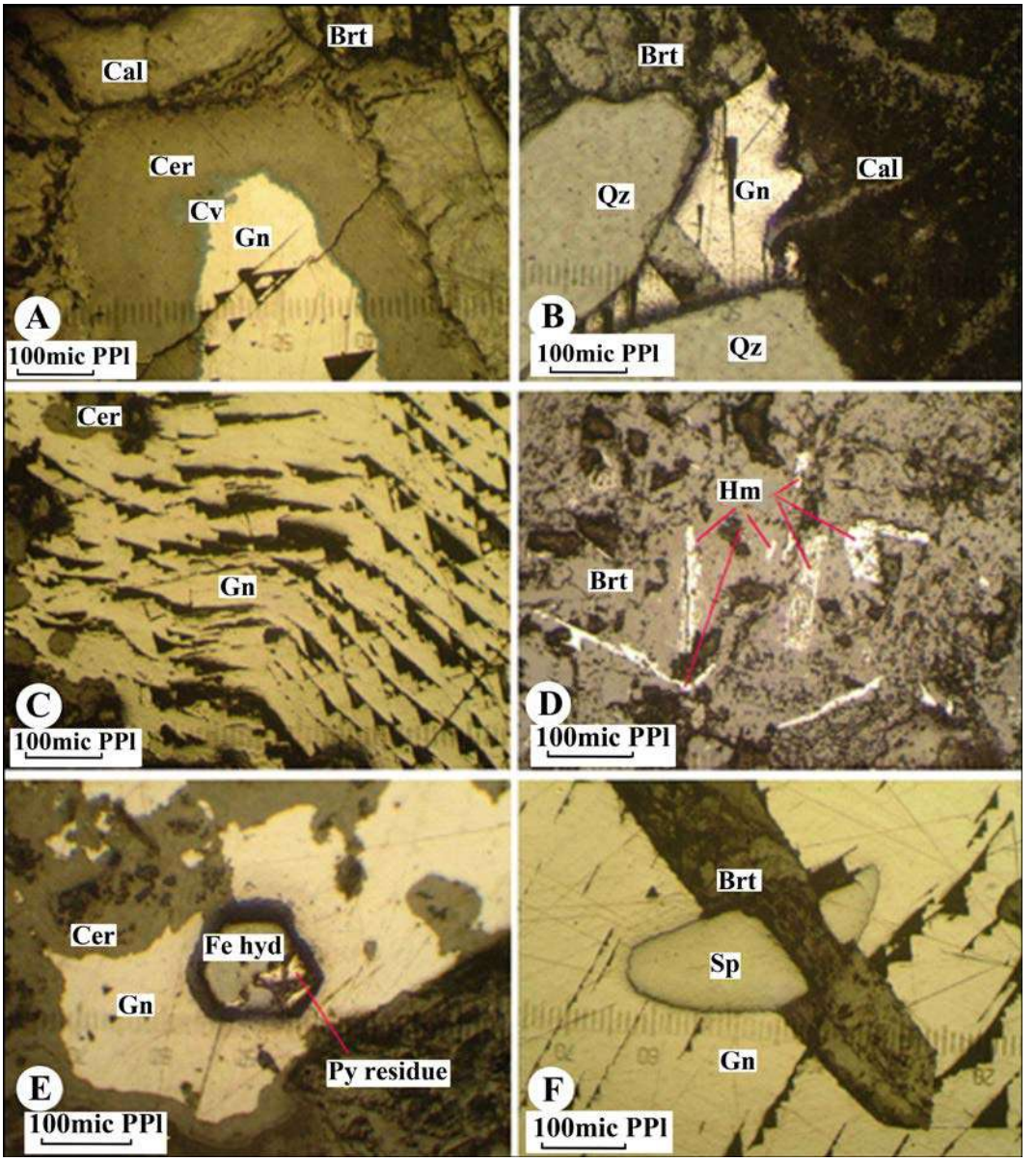

Text-fig. 11. Photomicrographs of minerals in the Duna mine. A – Aleration of galena to cerussite and covellite within the calcite and barite of discordant vein (DSa4) from open pit; B – Galena as filled veinlet of fractures between quartz, calcite and barite of concordant vein (DSa17) from tunnel; C – curved galena of concordant vein (DSa17) from tunnel; D – The Hematite blades in Barite of concordant vein (DSa7) from open pit; E – Alteration of crystalline euhedral pyrite to iron hydroxide and galena alteration from margins to cerussite of discordant vein (DSa1); F – The sphalerite inclusion in galena from discordant vein (DSa4) of open pit. Abbreviations: Brt – Barite; Cal – Calcite; Ccp – Chalcopyrite; Cv – Covellite; Gn – Galena; Hem – Hematite; Py – Pyrite; Qz – Quartz; Cer – Cerrussite; Sp – Sphalerite. Figures A and D are from open pit/mostly older/MVT, and figures B, C, E, and F are from tunnel/younger/Irish-type (symbols from Laurence (2021).

et al. 2003; Guest 2004; Guest *et al.* 2006; Hakimi Asiabar and Bagheriyan 2018), most of these faults formed after the Laramide tectonic phase. The fault arrays create hydraulic fractures and brecciated zones with pathways and conduits for hydrothermal fluids and other pressurized underground trapped fossil waters (Robb 2005). Hydrofracturing and hydrothermal breccia are also found in the Duna mine (Text-fig. 6E). The hydrothermal fluid flow also can create high hydraulic pressure. Fluid preferably flows along the brecciated zones associated with the main fault arrays. The mineralization map prepared in this work (Text-fig. 13) displays the relationship between faults and mineralization. Several mineralized veins occur

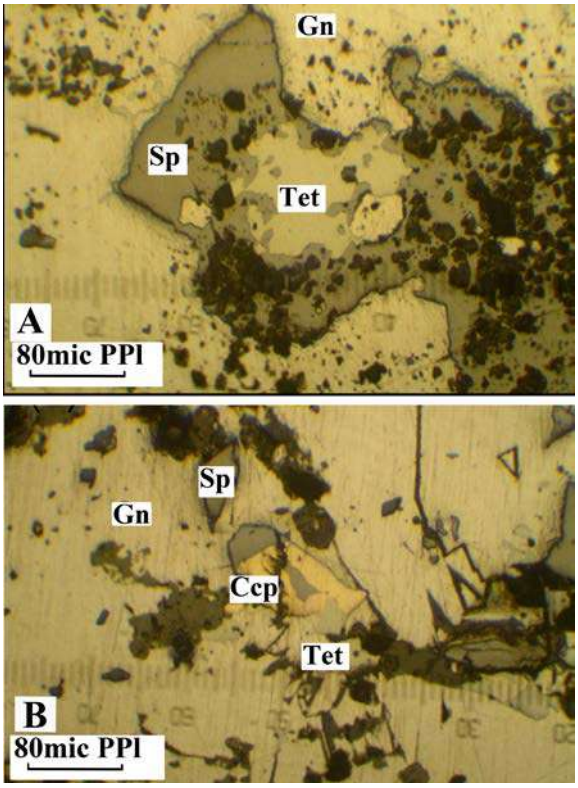

Text-fig. 12. Photomicrographs of minerals in the Duna mine. A – Replacement tetrahedrite (with Ag content), and sphalerite in galena of discordant vein (DSa1) from an open pit. B – Coprecipitation of sphalerite and chalcopyrite, and Replacement tetrahedrite, sphalerite, and chalcopyrite in galena of discordant vein (DSa1). Abbreviations: Ccp – Chalcopyrite; Gn – Galena; Sp – Sphalerite; Tet – Tetrahedrite (symbols from Laurence 2021).

along the <1 km-long strike-slip faults. Joints develop during folding. These joint sets can locally act as small-scale strike-slip faults with small slip magnitudes, especially on the hinterland side of thrust faults (Price 1966). Each generation of thrust fault usually accompanies some strike-slip faults, diagonal to its trend. The Northern Alborz deformed at least thrice after the Jurassic, especially during Late Cretaceous, Eocene–Oligocene and Pliocene (e.g., Axen *et al*. 2001b; Hakimi Asiabar and Bagheriyan 2018). These produced several small-scale strike-slip offsets. Even though mineralization along the strike-slip faults is abundant in the Duna mine, due to many complexities in crosscutting relationships, it is not useful to confirm the relative ages of ores with these fault arrays.

The Duna anticline is a part of a pop-up structure. According to the structural cross-sections (Text-fig. 4), several thrusts truncate the northern limb of the Duna east-plunging tight anticline. The geological cross-sections (Text-fig. 4B–D) display the relationship between mineralized zones, bedding of host rocks, fractures, and structural forms. In these cross-sections, some veins are concordant with sedimentary strata. All mineralized zones formed at the core of the Duna anticline and >95% of them occur in the Ruteh and Dorud Formations.

According to field data approximately 65% of the first-generation thrust faults with WSW-ESE trend, dip 40–50° (rake >60° to SE), and 45–55% of thrust faults with ~E-W trend, reverse movement (rake <50° to SE for the slip vector) contain mineralized zones (Text-figs 4, 5, 6).

Controlling factors of mineralization in the Duna mine

The most important mineralization controllers in Duna mine include: a) Once hydrocarbons transform into bitumen, their capability to chelate metal ions and sulfur diminishes (Ostendorf *et al*. 2015), and as a result, sulphide minerals, e.g., galena, sphalerite, and pyrite can deposit around the bituminous layers in the main mineralization stage (Ostendorf *et al*. 2015). Ore minerals in carbonate replacement systems typically consist of lead and zinc sulphides. The supergene minerals including Fe-oxy-hydroxides, cerussite, covellite, anglesite, malachite, and azurite, were formed by oxidation processes on the sulfide minerals near the surface. Anglesite ($PbSO_4$) has been widely identified as a supergene weathering product of primary galena in oxidation zones in supergene weathering deposits. Oxidation and acid-neutralization reactions partially dissociate the galena and promote the development of secondary supergene anglesite, which then surrounds and directly replaces the galena contained within the anglesite. The trap for carbonate-hosted lead-zinc sulphides can be a product of chemical reaction that occurs as a consequence of sulphur-concentration (Fusciardi *et al*. 2003), as zinc and lead are often absorbed by the hydrocarbons such as bituminous layers (Text-fig. 2). The hydrocarbons can either leak out of the fault zone or fold hinge, creating a stockwork of weakly mineralized carbonate-sulphide veins (Text-fig. 6F), or can degrade via pyrolysis in place to form bitumen (Ostendorf *et al*. 2015). b) Significant discordant mineralization of Pb, Ba, and Cu occurred over a horizon of limestone on the uppermost part of the Ruteh Formation and beneath the andesitic basalts of the Nessen Formation (Pab in Text-fig. 2). This mineralization is characterized by ore deposition in cavities, brecciated zones, and open spaces, e.g., vuggy and vesicle shapes, and as a result three main under-

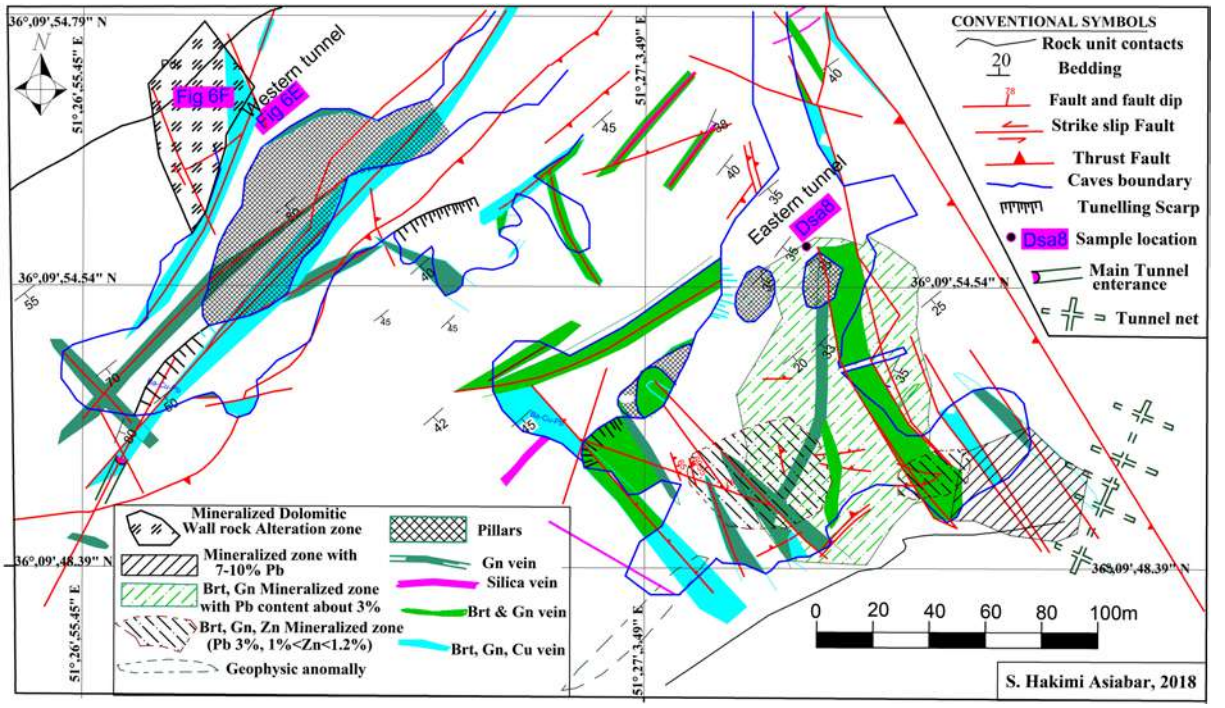

Text-fig. 13. The plan of mineralization in the eastern part of Duna mine, which displays the relation between faults and mineralization. Hatched shadow areas display scattered mineralized zones.

ground galleries and >1000 m long tunnels have been created for the excavation of mineralized zones by the miners (Text-fig. 13). Stratabound mineralization occurs in steeply-dipping Permian limestone and dolostones overlaid by a dense impermeable Melaphyr unit (Pab in Text-figs 2, 4) on the top level of the Duna anticline and controls the mineralization.

Fluid inclusions, geochemical features, and different types of mineralization in Duna mine

The integrity of fluid inclusion data is paramount in developing geofluid models that clarify the environmental conditions of fluid trapping (Feely 2018). The salinity versus homogenization temperature (Th°C) diagram (Wilkinson 2001) illustrates four types of fluid inclusions (Text-fig. 9B) in Duna mine; A) The first group consists of only a few fluids with ~7.44 wt.% NaCl equivalents and a homogenization temperature of 135–150°C. B) The second group of fluid inclusions has ~14–16 wt.% NaCl equivalent and a homogenization temperature of 180–225°C. These inclusions involved rapid precipitation of sulphides, driven by mixing between brines and higher temperature metal-bearing fluid derived from a basement-equilibrated fluid reservoir (Wilkinson and Eyre 2005). This category of fluid also can be created by mixing of a deep-seated, reducing, higher temperature, hydrothermal metal and possibly sulphur-bearing, and low-salinity fluid or a seawater-sourced, oxidizing, lower temprature, sulphur contributing high-salinity fluid, as described from the Lisheen Mine (Fusciardi et al. 2003). C) The third group consists of high-salinity fluid inclusions with 18.5–23.65 wt.% NaCl equivalent, and a homogenization temperature of 110–205°C. These fluids can come from seawater that evaporated to higher salinities and have precipitated halite (Banks *et al.* 2002) or can be created by bacteriologically produced H_2S (Wilkinson 2001). At the Duna mine, group B and C of fluid inclusions (Text-fig. 9D) are the same as the MVT deposit. D) The fourth group is fluid inclusions with medium to high-salinity (14.08–23.65 wt.% NaCl equivalent), and high homogenization temperature (250–285°C). This may indicate different formation conditions of discordant mineralized veins than the concordant mineralized veins (Sadeghi *et al.* 2022), and may indicate mineralization, at least spatially with igneous intrusions and saline springs (Banks *et al.* 2002), and as well it suggests that some magmatic and meteoric fluids were mixed (Arribas *et al.* 1995).

The general beliefs of a fluid inclusions study from the Irish-type ore deposit (Silvermines, Tynagh, and Navan ore deposits) suggest the role of two kinds of fluids (Wilkinson and Earls 2000) in the ore-forming process. The first type of fluid that carries metals in the Irish-type deposits has salinities ranging from 12 to 18 equivalent wt.% NaCl, while the homogenization temperatures range from 200°C to 250°C. The second type of fluid, presumably has a higher salinity of ~25 wt.% NaCl equivalent at a temperature <140°C. Fluids can mix partly in the subsurface, and partly when the hot metal-bearing fluid is exhaled into high-salinity magmatic or superficial water (Banks *et al*. 2002).

According to ICP-MS, the sample prepared from both concordant and discordant veins as shown in Table 1, includes the main elements in Duna mine. The average grade of the ore for concordant and discordant veins of mineralization is 19.5 and 18.1 wt. % Pb, 53.5 and 2541 ppm Zn, 81.1 and 146.6 ppm Ag, 26.1 and 1132.7 ppm As, 140 and 14310 ppm Cu, 53.8 and 3875 ppm Sb, 233 and 9200 ppm Sr, respectively. The high content of Ag, Cu, As, and Sb in the Duna mine which is associated with the Irish-type of mineralization is also very similar to the Pb-Zn deposits associated with magmatic activities (Leach *et al*. 2010).

DISCUSSION

The Early Cimmerian orogeny in the Alborz mountain range created an angular unconformity between the Jurassic and Triassic rock units. The Laramide orogenic movements caused overall marine regression, angular unconformity between Late Cretaceous and Cenozoic rock units, and folding, faulting, and inversion tectonics along previous normal faults, which in turn created numerous north- and south-verging thrust faults (Axen et al. 2001b; Allen et al. 2003; Guest et al. 2006). In the Eocene, another extension occurred with subsidence and remarkable eruptions in the Alborz range, with some magmatism, and continued with a Late Eocene–Oligocene compression. Inversion tectonics developed pop-up structures. A few researchers believe that the inversion tectonics of the Alborz range started by the end of the Mesozoic and continued up to the Neogene (Zanchi *et al*. 2006; Hakimi Asiabar *et al*. 2011; Ehteshami-Moinabadi 2016; Hakimi Asiabar and Bagheriyan 2018). The overall ongoing movement in the Alborz range is left-lateral slip (Axen *et al*. 2001b; Allen *et al*. 2003; Guest 2004; Guest *et al.* 2006; Ritz *et al*. 2006) as per the river offsets (Babaey *et al*. 2014; Javidfakhr and Ahmadian, 2019; Nazari *et al*. 2017). Changes in the deformation style of the Alborz range created some deformation in early formed structures in which new strike-slip faults developed.

Elevation-correlated (U-Th)/He age data from the Akapol suite indicate a 0.7 km My^{-1} rate of exhumation between 4 to 6 Ma (Axen *et al*. 2001b). This exhumation correlates well with the accelerated sedimentation in the south Caspian basin at ~ 6 Ma. Moreover ~ 10 km of subsidence in the Caspian basin can be assigned to loading by the Alborz mountains. Steep, dextral northwest-trending strike-slip faults in the Alamkuh region cut the Akapol granodiorite and are truncated by the Alamkuh pluton (Axen *et al*. 2001b). These results suggest that the change from Tertiary dextral strike-slip faulting to the presently observed sinistral strike-slip occurred as late as 7 Ma, possibly due to the Late Neogene onset of continental collision (Axen *et al*. 2001b).

The high-salinity and high-temperature of the fluid inclusions probably could have occurred by the end of Eocene as the Akapol plutonic body intruded (~ 10 km west and northwest of Duna mine and it has some stocks ~ 4 km south of the Duna mine), which in turn caused mixing with the saline springs such as at the Lisheen mine (Fusciardi et al. 2003). The fluid temperature of the Silvermine deposit is about 300ºC, which is the result of the influence of a mafic intrusive mass (Wilkinson and Hitzman 2015).

According to the isotopic ratios ($^{206}Pb/^{204}Pb$, $^{207}Pb/^{204}Pb$, $^{208}Pb/^{204}Pb$, $^{238}U/^{204}Pb$), the mineralization age of the Duna mine is ~ 50±6 Ma (Mirnejad *et al*. 2015) nearly synchronous with the intrusion of the Akapol granitoid (Sadeghi *et al*. 2022). The Akapol granodiorite intruded at 56±2 Ma, cooled to ~ 150°C by ~ 40 Ma, and resided at that temperature for at least 25 Ma. The persistence of ~ 150°C ambient conditions indicates tectonic stability for the Alamkuh region from Late Eocene up to Late Miocene (Axen *et al*. 2001b; Eshaghpour and Alizadeh Saloomahalleh 2015).

Comparison between MVT, Irish-type, and Duna type ore deposits

Table 4 compares the MVT, Irish-type, and Duna mine ore deposits. The characteristics of the Duna mine encouraged us to retry a comparison with MVT ore deposits. Chalcopyrite, bornite, and other Cu-bearing minerals are normally not constituents of the MVT deposits (Bortnikov *et al*. 1991), but in the Duna mine, chalcopyrite and chalcopyrite-sphaler-

Specification	Duna mine				Irish-type		MVT
F.I. categories	Group A	Group B	Group C	Group D	Group 1	Group 2	One Group
Th (°C)	132–150	180–225	110–205	250– 285	150–250	<140	50–150
NaCl wt. % eq.	7.44	14–16	18.5–24	21–24	12– 18	25	10–30
Form Reserve	concordant (stratabound) and discordant (faults and fractures infillings)				stratabound and stratiform		stratabound
Main minerals	galena, sphalerite, barite, chalcopyrite, tetrahedrite, covellite, pyrite				galena, sphalerite, barite, chalcopyrite, tetrahedrite		galena, sphalerite, barite, fluorite
Zn/Zn+Pb	0.02–0.2				>0.5		0.6–0.8 or >0.5
Ag (ppm)	160.8–264.3				<165		10 to 161
Metal content	Pb, Ba, Zn, Cu, Ag, Fe				Pb, Zn, Ag, Cu, Fe		Pb, Zn, Cd, Ge

Table 4. A comparison of mineralization characteristics between MVT (Paradis et al. 2007), Irish–type (Wilkinson 2001), and Duna type ore deposits from concordant and discordant veins. T_h°C – homogenization temperature; F.I. – fluid inclusion.

ite compounds are common (Text-fig. 12B) in some discordant mineralization zones, which indicate temperature conditions more than those of the MVT deposits. The Ag grade of the Duna mine is 16.8 to 264.8 ppm, and in a discordant vein in the tunnel there is an average of 1553 ppm (Sadeghi *et al*. 2022). but the silver content in MVT deposits varies from 10 to 161 ppm (Leach and Sangster 1993), and in some cases is not reported (Paradis *et al*. 2007). The Prairie Creek and Nanisivik deposits, with averages of 161 and 34 g t^{-1} Ag, respectively, have the highest silver grades of MVT deposits in Canada (Leach and Sangster 1993; Paradis *et al*. 2007). The Duna deposit is zinc-poor relative to lead and has a Zn/(Zn+Pb) ratio of <0.1, but most MVT deposits in Canada are zinc-rich relative to lead and have > 0.5 magnitudes of that ratio (Paradis *et al*. 2007). Few deposits in east Tennessee and the Newfoundland district are essentially free of lead and have Zn/(Zn+Pb) ratios ~ 1 (Leach and Sangster 1993).

It seems that the Cu content of the Duna Pb-Ba ore deposit in some veins is more than or equal to that of the Zn content. There is a general enrichment of Ag around the feeders of Irish Pb-Zn deposits (Banks *et al*. 2002). Higher temperature mineralization, including the Cu, Ag bearing phases, occurred nearest the sources of the higher temperature fluids, and Andrew (1986) suggested that the late Cu-bearing stage of mineralization at Tynagh was possibly related to the Cu-Ag deposits. These Cu-Ag deposits, e.g., that at Gortdrum (Ireland), appear to be associated with igneous intrusions (Banks *et al.* 2002). The high-temperature mineralization at Lisheen occurred during the early part of the main Zn-Pb phase (Fusciardi et al. 2003). Copper is insoluble at significant concentrations in ore fluids of moderate temperature (160–180°C) and salinity (9–15 wt.% NaCl equivalent) until the temperature reaches ~300°C (Ixer 2003). Cu, Ag-bearing, and other high-temperature sulphides occur deeper in the mineralizing systems, exhibiting more vein-type forms (Andrew 1986; Doyle *et al*. 1992). Some trace elements such as Cu, As and Sb in the Duna mine are similar to the Irish type and tomagmatic Pb-Zn deposits (Leach *et al*. 2010; Sadeghi *et al*. 2022).

Genetic model of main mineralization types in the Duna mine

The geometry scheme of fractures, especially in the forelimb of the Duna anticline indicates that this anticline formed in the first deformation stage after the Shemshak Formation existed. Later the fold was affected by thrusts. Study of angular unconformities and geologic settings proves that after the sedimentation of the Shemshak Formation, a major folding phase commenced and continued with thrusting to the end of Cretaceous, which was later loaded with hydrothermal fluids and mineralized zones. In the study area, the Shemshak Formation deformed entirely within the Paleozoic and Triassic rock units. Thus, the first evolving stage of the Duna anticline commenced by the Late Cretaceous. The crosscut relation between major thrust faults and folds represents the Laramide and Pyrenean ages for discordant types of mineralization along thrust faults. Evaluation of our structural data, fluid inclusion, dating of the Duna mine (Rajabi *et al*. 2013), and Akapol intrusions (Sajadi Nasab *et al*. 2014) encapsulate the mineralization (Text-fig. 14B–E). The Duna ore deposit is situated in a rhombic asymmetric pop-up structure (Text-fig. 14C–E), and the faults are curved in plain view (Text-fig. 14F). Such strike-slip fault systems can produce localized zones of extension and subsidence, whereas localized zones of contraction usually produce stopovers or pop-ups for the restraining stopovers (Mc Clay and Bonora 2000). In cross-sections, the pop-ups are dominantly asym-

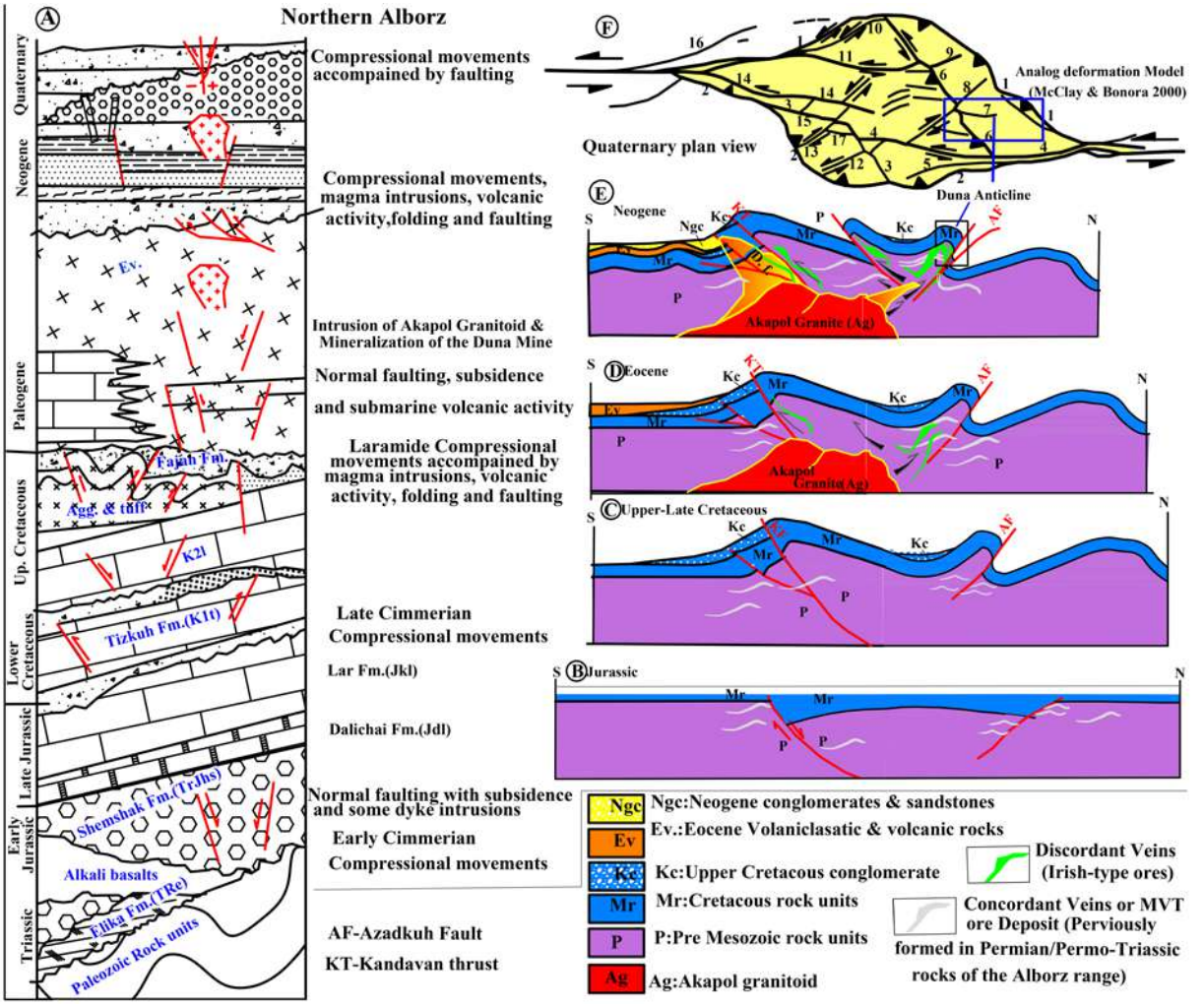

Text-fig. 14. A – The tectonostratigraphic chart (modified after Hakimi Asiabar and Bagheryian 2018) of the Northern Alborz range. B, C, D, and E – A schematic model for the deformation processes of the Duna mine (faults, folding, and Akapol intrusive). F – Analog deformation model (Mc Clay and Bonora 2000).

metric with the bounding faults dipping inward into the basement fault systems (Text-fig. 14F). The progressive evolution of strike-slip pop-up structures in plain view with increased displacement on the basement fault systems in early formed uplifted areas gets these dissected, fragmented, and transported, along with the major strike-slip system. Changes in deformation style of the Alborz range during the Neogene and Quaternary also created some deformation in the early formed structures, with new strike-slip faults, localized zones of extension and subsidence, stopovers, or pop-ups for restraining stopovers such as the structures and analog models of Mc Clay and Bonora (2000). These movements can also rotate the previously formed anticlines.

As per analogue models, some high-angle reverse faults (fault 6 in Text-fig. 14F) can emerge in internal parts of these types of pop-up structures (Mc Clay and Bonora 2000). Natural pop-ups that display similar morphological features and structures have been reported from the Cerro de la Mica, Atacama strike-slip fault system, northern Chile (Mc Clay and Bonora 2000), and the Owl Creek, Wyoming, USA (Paylor and Yin 1993). It seems that the orogenic phases of the Late Cretaceous and Cenozoic and the intrusion of plutonic bodies influenced the previously formed MVT ore deposit and overprinted mineralization during the Cenozoic. Evolving fluids with homogenization temperature ~250–285°C as shown by samples taken from brecciated zones

(samples DSa4, DSa8 in Text-fig. 9B) probably are evidence of magmatic involvement in the mineralization history. Mineralization along the first and second generations of thrust faults demonstrates the overlapping of ore-forming events at Duna Pb-Ba ore deposit, predated to the Neogene and Quaternary latest faulting episode, which in turn was controlled by the Duna anticline and lithology of the surrounding rocks. Stratabound, carbonate-hosted and sulphide mineralization of MVT deposits was mostly formed as concordant veins in Permian and Triassic periods. These deposits can originate from saline basinal metalliferous fluids at 75–200°C (Leach and Sangster 1993; Wilkinson 2001; Paradis *et al.* 2007). This concordant type of mineralization of Permian–Triassic carbonate-hosted Zn-Pb ore deposits are common in Central Iran and the Alborz range (Rajabi *et al*. 2013) and goes back to the MVT ore deposit.

CONCLUSIONS

- This work introduces a new class of mineralization in the Alborz region*;* the *Duna type ore deposit,* with four groups of fluid inclusions, homogenization temperatures and salinity ranges from 110–285°C and 7.34-23.65 wt.% NaCl equivalent respectively, Zn/Zn+Pb ratio <0.1, and high content of Ag (>200 ppm).
- The MVT deposit stage of the Alborz range formed during the early stages of deformation and was rejuvenated by the intervention of tectonic episodes and intrusion of Eocene plutonic bodies. The rejuvenation phase was confirmed by high-salinity high-temperature types of fluid inclusions which can be created by the Irish-type of mineralization.
- Three major thrust fault generations are recognized in the study area. Mineralization happened along the first and second generations of thrust faults arrays. This indicates that the ore-forming events predate the third faulting episode.
- Mineralization in the Duna Pb-Ba ore deposit was structurally controlled by the Duna anticline, faults, and chemically affected by the bituminous layers, dolomitic horizons, and impermeable Permian volcanic rocks.
- Correlation of structural data, fluid inclusions, age of the Duna Pb-Ba ore deposit, and Akapol plutonic intrusions show at least two major overprinted mineralization phases with concordant (Early Cimmerian) and discordant (Late Cretaceous and Cenozoic) forms of mineralization.

Acknowledgments

We would like to thank Mr. Amin Akrami and Mr. Arash Mirshahi, the Chief Executives of the Damavand Mining Project for sharing information. This research did not receive any specific grant from funding agencies in the public, commercial, or not-for-profit sectors. CPDA grant (IIT Bombay) supported SM. Also thanks to reviewers, and proofreaders for their efforts.

REFERENCES

Aghanabati, A. 2005. Geology of Iran. 733 pp. Geological Survey of Iran Publication. Tehran.

Aerden, D., Sayab, M. and Bouybaouenel, M. 2010. Conjugate-shear folding: A model for the relationships between foliations, folds, and shear zones. *Journal of Structural Geology*, **32**, 1030–1045.

Allen, M., Ghassemi, M.R., Shahrabi, M. and Qorashi, M. 2003. Accommodation of late Cenozoic oblique shortening in the Alborz range, northern Iran. *Journal of Structural Geology*, **25**, 659–672.

Andrew, C.J. 1986. The tectonostratigraphic controls to mineralization in the Silvermines area, County Tipperary, Ireland. In: Andrew C.J., Crowe R.W.A., Finlay S., Pennell, W.M., Pyne J. (Eds), Geology and Genesis of Mineral Deposits in Ireland, 377–408. Irish Association for Economic Geology; Dublin.

Annells, R.N. 1975. Explanatory text of the Qazvin and Rasht quadrangles map. 94pp. Geological Survey of Iran.

Arribas, A.J.R., Cunningham, C.G., Rytuba, J.J., Rye, R.O., Kelly, C., Podwysocki, M.H., Mckee, E.H. and Tosdal, R.M. 1995. Geology, geochronology, fluid inclusions and isotope geochemistry of the Rodalquilar Au alunite deposits, Spain. *Economic Geology*, **90**, 795–822.

Axen, G.J., Lam, P.S., Grove, M., Stockli, D.F. and Hassanzadeh, J. 2001b. Exhumation of the West-Central Alborz Mountains, Iran, Caspian subsidence, and collision-related tectonics. *Geology*, **29**, 559–562.

Babaey, S., Dehbozorgi, M. and Hakimi Asiabar, S. 2014. Assessment of active tectonics by using morphometric indices in Central Alborz. *Quarterly Quantitative Geomorphological Research*, **1**, 40–56.

Baharfiruzi, Kh. and Shafeii, A.R. 2005. Geological map of Javaherdeh (1:100,000) sheet. Geological Survey of Iran, Tehran, Iran.

Banks, D.A., Boyce, A.J. and Samson, I.M. 2002. Constraints on the origins of fluids forming Irish Zn-Pb-Ba deposits: Evidence from the composition of fluid inclusions. *Economic Geology*, **97**, 471–480.

Bazargani-Gilani, K. 1982. Die mittelpermischen Scichtgebundenen Blei-Zink-Schwerspat-Largestattendes Kalawanga Distriktes. Zentral Alborz, Iran (mit besonderer Berucksich-

tigung des Duna-Grubenfelds), 163 pp. Ph.D. Thesis, Diss university, Heidelberg.

Bean, R.E. 1983. The Magmatic-Meteoric Transition. In: Armstrong, R.L. (Ed.), The Role of Heat in the Development of Energy and Mineral Resources in the Northern Basin and Range Province. *Geothermal Resources Council, Special Report*, **13**, 245–253. Davis, California.

Bortnikov, N.S., Genkin, A.D., Dobrovol'skaya, M.G., Muravitskaya, G.N. and Filimonova, A.A. 1991. The nature of chalcopyrite inclusions sphalerite: Exsolution, coprecipitation, or "disease"? *Economic Geology*, **86**, 1070–1082.

Doyle, E., Bowden, A.A., Jones G.V., and Stanley, G.A. 1992. The geology of the Galmoy zinc-lead deposits, Co. Kilkenny. In: Bowden, A.A., Earls, G., O.'Connor, P.G. and Pyne, J.F. (Eds), The Irish Minerals Industry 1980–1990, 211–225. Irish Association for Economic Geology; Dublin.

Ehteshami-Moinabadi, M. 2016. Possible basement transverse faults in the Western Alborz, northern Iran. *Journal of Sciences, Islamic Republic of Iran*, **27**, 329–342. [In Persian]

Eshaghpour, M. and Alizadeh Saloomahalleh, H. 2015. Relationship between thermal springs of Western Alborz Mountains and regional tectonics. *Proceedings of World Geothermal Congress, Melbourne, Australia, 19–25 April 2015*, 9 pp. University of Melbourne; Melbourne.

Feely, M. 2018. Editorial for special issue. Fluid inclusions: Study methods, applications, and case histories. *Minerals*, **8**, 307–309.

Fusciardi, L.P., Guven, J.F., Stewart, D.R.A., Carboni, V., Walsh, J.J. 2003. The geology and genesis of the Lisheen Zn-Pb deposit, Co. Tipperary, Ireland. In: Kelly, J.G., Andrew, C.J., Ashton, J.H., Boland, M.B., Earls, G., Fusciardi, L. and Stanley, G. (Eds), Europe's Major Base Metal Deposits, 455−481. Irish Association for Economic Geology; Dublin.

Goldstein, R.H. and Reynolds, T.J. 1994. Systematics of fluid inclusion in diagnostic minerals. 199 pp. Society of Economic Geologists and Paleontologists.

Guest, B. 2004. The thermal, sedimentological, and structural evolution of the Central Alborz Mountains of northern Iran: Implications for the Arabia-Eurasia continent-continent collision and collisional processes in general Ph.D. thesis. 292 pp. University of California; Los Angeles.

Guest, B., Axen, G.J., Lam, P.S. and Hassanzadeh, J. 2006. Late Cenozoic shortening in the west-Central Alborz Mountain, northern Iran, by combined conjugate strike-slip and thin-skinned deformation. *Geosphere*, **2**, 35–52.

Hakimi Asiabar S., Pourkermani M., Shahriari S., Ghorbani M. and Ghasemi M.R. 2011. Geological zones of western Alborz Mountains. *Journal of Sciences, Islamic Azad University*, **21**, 113–124.

Hakimi Asiabar, S. and Bagheriyan, S. 2018. Exhumation of the Deylaman fault trend and its effects on the deformation style of the western Alborz belt in Iran. *International Journal of Earth Sciences*, **107**, 539–551.

Hakimi Asiabar, S. 2019. Structural deformations of Duna mine. *Scientific Quarterly Journal, Geosciences*, **28**, 235–246. [In Persian]

Hashemian, E., Jamali, H. and Ahmadian, J. 2018. Mineralogy, Fluid inclusion and Geochemistry of Tappeh-Khargosh Cu-Au deposit (SW of Ardestan), Iran. *Journal of Economic Geology*, **10**, 299–324.

Hassanzadeh, J., Ghazi, A.M., Axene, G., Guest, B., Stocklin, D. and Tucker, P. 2002. Oligocene mafic-alkaline magmatism in north and northwest of Iran: Evidence for the separation of the Alborz from the Urumieh-Dokhtar magmatic arc. *Geological Society of America, Abstracts with Programs* **34** (6), 331.

Holzer, H.F. and Momenzadeh, M. 1969. Note on the geology of Elika and Duna lead mines, Central Alborz, northern Iran. *Geological Survey of Iran*, **21**, 27–36.

Ixer, R.A. 2004. The petrography of the zinc-lead-copper ores at Crow Island, Killarney, Ireland. *UK Journal of Mines and Minerals*, **24**, 29–34.

Jackson, J., Priestley, K., Allen, M. and Berberian, M. 2002. Active tectonics of the South Caspian Basin. *Geophysical Journal International*, **148**, 214–245.

Javidfakhr, B. and Ahmadian, S. 2019. Structural concepts for Soltanieh fault zone (NW Iran). *Iranian Journal of Earth Science*, **11**, 290–304.

Laurence, N.W. 2021. IMA-CNMNC approved mineral symbols. *Mineralogical Magazine*, **85**, 291–320.

Leach, D.L. and Sangster, D.F. 1993. Mississippi Valley-type lead-zinc deposits. In: Kirkham, R.V., Sinclair W.D., Thorpe R.I. and Duke, J.M. (Eds), Mineral Deposit Modeling. *Geological Association of Canada Special Paper*, **40**, 289–314.

Leach, D.L., Bradley, D.C., Huston, D., Pisarevsky, S.A., Taylor, R.D. and Gardoll, S.J. 2010. Sediment-hosted lead-zinc deposits in Earth's history. *Economic Geology*, **105**, 593–625.

Lisle, R.J. 1986. The sectional strain ellipse during progressive coaxial deformations. *Journal of Structural Geology*, **8**, 809–817.

Mc Clay, K. and Bonora, M. 2000. Analogue models of restraining stopovers in strike-slip fault systems. *AAPG Bulletin*, **85**, 233–260.

Mirnejad, H., Simonetti, A. and Molasalehi, F. 2015. Origin and formational history of some Pb-Zn deposits from Alborz and central Iran: Pb isotope constraints. *Journal of International Geology Review*, **57**, 463–471.

Mitra, S. 2003. A unified kinematic model for the evolution of detachment folds. *Journal of Structural Geology*, **25**, 1659–1673.

Modaresnia, M., Khosrotehrani, K., Momeni, I. and Babazadeh, S.A. 2012. Upper Cretaceous planktonic foraminiferal biostratigraphy of east Dorfak area (Guilan – north of Iran). *Life Science Journal*, **9**, 242–253.

Mukherjee, S. 2013. Deformation Microstructures in Rocks. 112 pp. Springer Science & Business Media; Berlin.

Mukherjee, S. 2014. Review of flanking structures in meso- and micro-scales. *Geological Magazine*, **151**, 957–974.

Mukherjee, S. 2015. Atlas of Structural Geology. 165 pp. Elsevier.

Nazari, H., Ritz, J.F., Walker R.T., Salamati R., Rizza M. and Patnaik R. 2014. Paleoseismic evidence for a medieval earthquake, and a preliminary estimate of late Pleistocene slip-rate, on the Firouzkuh strike-slip fault in the Central Alborz region of Iran. *Journal of Asian Earth Sciences*, **82**, 124–135.

Nekouvaght Tak, M., Bazargani-Guilani. K. and Framarzi, M. 2009. Geology and Geochemistry of the lead-zinc carbonated hosted MVT mineralization in the north Semnan. Central Alborz., Iran. In: Procceding of 10th Biennial SGA Meeting Townsville, 499–501. Economic Geology Research Unit, James Cook University; Australia.

Ostendorf, J., Henjes-Kunst, F., Mondillo, N., Boni, M., Schneider, J. and Gutzmer, J. 2015. Formation of Mississippi Valley-type deposits linked to hydrocarbon generation in extensional tectonic settings: Evidence from the Jabali Zn-Pb-(Ag) deposit (Yemen). *Geology*, **43**, 1055–1058.

Paradis, S., Hannigan, P., and Dewing, K. 2007. Mississippi Valley-type lead-zinc deposits (MVT). In: Goodfellow, W.D. (Ed.), Mineral Deposits of Canada: A Synthesis of Major Deposit-Types, District Metallogeny, the Evolution of Geological Provinces, and Exploration Methods. *Geological Association of Canada, Mineral Deposits Division, Special Publication*, **5**, 185–203.

Paylor, E.D. and Yin, A.N. 1993. Left-slip evolution of the North Owl Creek fault system, Wyoming, during Laramide shortening. In: Christopher J. Schmidt, Ronald B. Chase and Eric A. Erslev (Eds), Laramide basement deformation in the Rocky Mountain foreland of the western United States. *Geological Society of America Special Papers*, **280**, 229–242.

Price, N.J. 1966. Fault and Joint Development in Brittle and Semi-Brittle Rock. 186 pp. Pergamon Press; New York.

Rajabi, A., Rastad, E. and Canet, C. 2013. Metallogeny of Permian–Triassic carbonate-hosted Zn-Pb and F deposits of Iran: A review for future mineral exploration. *Australian Journal of Earth Sciences*, **60**, 197–216.

Ritz, J.F., Nazari, H., Ghassemi, A., Salamati, R., Shafei, A., Solaymani, S. and Vernant, P. 2006. Active transtension inside Central Alborz: A new insight into northern Iran–southern Caspian geodynamics. *Geology*, **34**, 477–480.

Robb, L.J. 2005. Introduction to Ore-forming processes. 373 pp. Blackwell Publishing Australia; Carlton, Victoria.

Roedder, E. 1984. Fluid inclusions. *Reviews in Mineralogy, Mineralojical Society of America*, **12**, 644.

Sadeghi, A., Nezafati, N., Hakimi Asiabar, S. and Ganji, A. 2022. Geological, geochemical and fluid inclusion investigations on the Duna Pb-Ba-(Ag) deposit, Central Alborz, North Central Iran. *Geologia Croatica*, **75**, 145–163.

Sajadi Nasab, M.A., Vosoughi Abedini, M., Emami, M.H. and Ghorbani, M. 2014. Petrogenesis of the Akapol Granitoidic intrusion, Kelardasht area, Central Alborz, Iran. *Scientific Quarterly Journal*, *Geosciences*, **23**, 241–252.

Samanirad, A. 1999. Geology, petrology and genesis of Duna Lead deposit in the Central Alborz, 125 pp. Unpublished M.Sc. Thesis, Islamic Azad University; Tehran. [In Persian]

Shepherd, T.J., Rankin, A.H. and Alderton, D.H.M. 1985. A Practical Guide to Fluid Inclusion Studies. 239 pp. Chapman and Hall, New York.

Steele-Macinnis, M., Bodnar, R.J. and Naden, J. 2011. Numerical model to determine the composition of H_2O-NaCl-$CaCl_2$ fluid inclusions based on microthermometric and microanalytical data. *Geochimica et Cosmochimica Acta*, **75**, 21–40.

Wilkinson, J.J. and Earls, G. 2000. A high-temperature hydrothermal origin for black dolomite matrix breccias in the Irish Zn-Pb orefield. *Mineralogical Magazine*, **64**, 1077–1096.

Wilkinson, J.J. 2001. Fluid inclusion in hydrothermal ore deposits. *Lithos*, **55**, 229–272.

Wilkinson, J.J. and Eyre, S.L. 2005. Ore-forming processes in Irish-type carbonate-hosted Zn-Pb deposits: Evidence from mineralogy, chemistry, and isotopic composition of sulphides at the Lisheen mine. *Economic Geology*, **100**, 63–86.

Wilkinson, J.J. and Hitzman, M.W. 2015. The Irish Zn-Pb Orefield: The view from 2014, 59–69. Irish Association for Economic Geology, Geological survey of Irland; Dublin.

Yaghoobpour, M. 2004. Investigation of geochemical, Isotopic and fluid inclusion related to the source Pb-Zn ore deposit in Duna, 136 pp. M.Sc. Thesis, Shomal University; Tehran.

Zanchi, A., Berra, F., Mattei, M., Ghassemi, M.R. and Sabouri, J. 2006. Inversion tectonics in Central Alborz, Iran. *Journal of Structural Geology*, **28**, 2023–2037.

Manuscript submitted: 6th June 2022
Revised version accepted: 17th November 2022